Journal of Dentistry 143 (2024) 104906

Contents lists available at ScienceDirect

Journal of Dentistry

journal homepage: www.elsevier.com/locate/jdent

Characterisation of experimental flowable composites containing fluoride-doped calcium phosphates as promising remineralising materials

Adrián M. Alambiaga-Caravaca [a,b], Yu Fu Chou [c], Daniel Moreno [d], Conrado Aparicio [d,e], Alicia López-Castellano [a], Victor Pinheiro Feitosa [f], Arzu Tezvergil-Mutluay [g], Salvatore Sauro [c,*]

[a] Department of Pharmacy, Faculty of Health Sciences, Institute of Biomedical Sciences, Cardenal Herrera-CEU University, CEU Universities, Valencia, Spain
[b] Department of Anatomy & Regenerative Medicine, Tissue Engineering Research Group, Royal College of Surgeons in Ireland, Dublin, Ireland
[c] Department of Dentistry (Dental Biomaterials and Minimally Invasive Dentistry), Faculty of Health Sciences, Univeristy CEU Cardenal Herrera, CEU Universities, Alfara del Patriarca, Valencia 46115, Spain
[d] Division of Research, Faculty of Odontology, UIC Barcelona – Universitat Internacional de Catalunya, Sant Cugat del Vallès, Barcelona, Spain
[e] IBEC-Institute for Bioengineering of Catalonia, Barcelona, Spain
[f] Department of Operative Dentistry, College of Dentistry, University of Iowa, Iowa City, USA
[g] Adhesive Dentistry Research Group, Institute of Dentistry, and TYKS University Hospital, University of Turku, Turku, Finland

ARTICLE INFO

Keywords:
Remineralisation
Ion-release
Antibacterial
Calcium phosphate
Resin composite
Apatite

ABSTRACT

Objective: Remineralising composites with antibacterial properties may seal the cavity and prevent secondary caries. This study aimed at developing experimental flowable composites containing different concentrations of fluoride-doped calcium phosphate fillers and evaluating their remineralising and antibacterial properties.
Methods: Experimental resin-based composites containing different concentrations (0–20 %) of fluoride-doped calcium phosphate fillers (VS10/VS20) were formulated. The release of calcium (Ca), phosphate (PO) and fluoride (F) ions was assessed for 30 days. Remineralisation properties were evaluated through ATR-FTIR and SEM/EDX after storage in simulated body fluid (SBF). The metabolic activity and viability of *Streptococcus gordonii* was also evaluated through ATP, CFU and live/dead confocal microscopy. The evaluation of specific monomer elution from the experimental composites was conducted using high-performance liquid chromatography (HPLC).
Results: The composites containing VS10 showed the highest release of Ca, those containing VS20 released more F over time ($p < 0.05$), while there was no significant difference in terms of PO ions release between the groups ($p > 0.05$). A quick 7-day mineral precipitation was observed in the tested composites containing VS10 or VS20 at 10 %; these materials also showed the greatest antibacterial activity ($p < 0.05$). Moreover, the tested composites containing VS10 presented the lowest elution of monomers ($p < 0.05$).
Conclusions: Innovative composites were developed with low monomers elution, evident antibacterial activity against S. gordonii and important remineralisation properties due to specific ions release.
Clinical significance: Novel composites containing fluoride-doped calcium phosphates may be promising to modulate bacteria growth, promote remineralisation and reduce the risk of cytotoxicity related to monomers' elution.

1. Introducion

The key aim in minimal invasive dentistry is to maintain patients' teeth healthful and functional as long as possible, through specific preventive and operative strategies; risk assessment and early caries detection represent the first pillars of such a therapeutic philosophy [1,2]. In presence of early caries lesions in enamel, remineralisation along with other preventive treatments should be immediately employed to stop the progression of the demineralisation. Whereas, once the caries lesion has invaded the dentine substrate, minimally invasive operative interventions such as selective carious tissue removal should be prioritised for cavity preparation, especially in deep lesions adjacent to the pulp [3,4]. Indeed, there is a constant increase in evidence that such a clinical approach can reduce the risk pulp exposure in deep cavities [5,

* Corresponding author.
E-mail address: salvatore.sauro@uch.ceu.es (S. Sauro).

https://doi.org/10.1016/j.jdent.2024.104906
Received 4 February 2024; Received in revised form 24 February 2024; Accepted 26 February 2024
Available online 28 February 2024

6], and improve the longevity of the treated teeth, as far as restorations are able to seal the caries-affected cavity adequately and prevent secondary caries [7,8]. Unfortunately, secondary caries in composite restorations even represent a critical issue in restorative dentistry [9].

This seems to be due to in part to some critical chemical-morphological characteristics of adhesive composite restoration, as for instance the inability of resin bonding systems to completely infiltrate and/or "repair" the mineral-depleted caries-affected dentine [10,11]. Indeed, the collagen fibrils that remain devoid of resin-encapsulation can degrade over time and reduce the longevity of composite restorations [12–14]. It is advocated that a realistic approach to restoring such a demineralised dentine substrate is represented by the use of materials with remineralisation and antibacterial properties [6,7]. Among the materials currently available on the market to restore teeth after selective caries removal there are calcium silicate, conventional glass ionomer (GICs) and resin-modified glass ionomer (RMGIC) cements. It has been widely demonstrated that such materials can be used as dentine replacement material for their specific mechanical properties, as well as materials able to induce increase in mineral gain when in contact with demineralised dentine [14–16]. Unfortunately, none of such materials available on the market are able to effectively "repair" caries-affected dentine [11,14,17]. Hence, there is a definite need to develop innovative restorative ion-releasing materials able to interact with dental hard tissues and biological fluids (e.g. saliva) and seal adequately the dentine-restoration interface [11,18]. Furthermore, one of the main objectives of several dental materials scientists, as well as dental industries, is to develop restorative materials that have the characteristic to prevent bacteria colonisation and penetration of pathogen-associated molecular complexes [8,19,20].

In this regard, experimental resin-based calcium-phosphate cements have been advocated as potential therapeutic materials due to their ability to remineralise caries-affected dentine [21]. More recently, some calcium phosphates tailored with different concentrations of fluoride salts have been demonstrated to convert into biocompatible fluoride-containing apatite-like crystals when immersed in simulated body fluid; such promising ion-releasing resin-based materials might be able to preserve the longevity of restorations performed after caries removal [22].

Thus, this *in vitro* study aimed at developing a number of experimental resin-based flowable composites containing different concentrations of fluoride-doped calcium phosphate fillers and evaluating their remineralising and antibacterial properties. This aim was accomplished by assessing the cumulative amount of calcium (Ca), phosphate (PO) and fluoride (F) released at standard condition (deionised water) up to a period of 30 days. A crystallographic assessment on the surfaces of the experimental composites through Fourier-transform infrared spectroscopy (ATR-FTIR), ultra-high-resolution analytical focused ion beam scanning electron microscopy and energy dispersion-type x-ray spectroscopy (FIB-SEM/EDX) was also performed to evaluate their mineralisation ability over a period of storage of 30 days in simulated body fluid (SBF). Moreover, in order to evaluate the antibacterial properties of the tested experimental composites, the metabolic activity of *S. gordonii* was evaluated with Adenosine triphosphate (ATP) and bacteria viability with a combination of colony forming units measurements (CFU) and LIVE/DEAD imaging. Finally, the release of urethane dimethacrylate (UDMA), 1.6-hexanediol ethoxylate diacrylate (HEDA) and ethoxylated bisphenol-A dimethacrylate (Bis-EMA) from the experimental composites was also evaluated through high-performance liquid chromatography.

2. Materials and methods

2.1. Specimen preparation - pH and ions release evaluation

Fluoride-doped calcium phosphate (FDCP) fillers were formulated as previously reported in literature [22]. In brief, a 1:1 molar ratio of beta-tricalcium phosphate (α-TCP) and monocalcium phosphate monohydrate (MCPM), calcium hydroxide (10 wt.%), calcium and sodium fluoride salts (1:1 molar ratio) at different concentrations (VS10:10 wt. % or VS:20 wt.%) were mixed with deionised water and subsequently milled and sieved (particle size < 50 μm). Two FDCP fillers were used in this study (VS10 and VS20) to generate six experimental flowable composites. In order to accomplish such a target, FDCP fillers were dispersed at different concentrations (5 vol%; 10 vol%; 20 vol%) in a resin bland made of 55 wt% UDMA, 20 wt% Bis-EMA, 25 wt% HEDA. Camphoroquinone and ethyl 4-dimethylaminobenzoate were incorporated at 1 mol%, while trimethylbenzoyl-diphenylphosphine oxide, and 2.4 dihydroxybenzophenone were used at 0.5 mol%. Butylated hydroxytoluene (0.01 wt%) was also used as a stabiliser. A nanofiller (AEROSIL® R972, Evonik Industries AG, Essen, Germany), a form of fumed silica with an average diameter of 16 μm, was also added at 26 wt %. All these components, as well as the experimental VS fillers were mixed at a rate of 60 rpm in an overhead stirrer mixer at 50 °C up to obtain a homogeneous composite mixture. This final composite was used as control composite (CTR), while the experimental composites containing the FDCP filler VS10 or VS20 were: VS10-5 %; VS10-10 %; VS10-20 %; VS20-5 %; VS20-10 %; VS20-20 %. All chemical reagents were purchased from Merck Life Science SLU (Madrid, Spain).

Five specimens were prepared for each tested material. Disk-shaped silicone moulds (8 × 2.5 mm= 1.66 cm^2) were positioned over a glass slide that was previously covered with a thin Mylar strip and the tested composites were directly dispensed into the moulds and immediately covered with a Mylar strip, which was manually pressed with another 1.0 mm-thickness glass slide. The polymerisation was achieved through light-curing for 30 s each side using a LED light curing unit (1200 mW/cm^2), (Radii Plus. SDI Ltd. Bayswater VIC. Australia), placing the light tip in contact with the glass slide. The specimens were then removed from the matrix and the specimens were carefully polished using a 600-grit SiC paper under constant irrigation and finally immersed in 20 ml deionised water.

The pH of the storage solution was measured using a pH meter (Hach Sens Ion+. SN: 705013. Hach-Langg SLU), while fluoride-release was measured using a direct potentiometry method with a liquid membrane for selective fluoride-ion electrode up to 30 days (30d). Before starting the measurements, the electrode was rinsed with deionised water and allowed to stand with the electrode conditioning solution (Conditioning Solution FI-SA-100 mL) for 10 min. Standard fluoride-containing solutions (1 mg L^{-1}, 5 mg L^{-1}, 10 mg L^{-1}, 50 mg L^{-1} and 100 mg L^{-1}) were used for the calibration of the Ion (Fluoride)-selective electrode (ISE. NT-F-MD019), using the reference electrode Ag/AgCl (SK-402–75B-CR) by XS 80 DHS (XS Instruments, Italy) [23]. After each reading, the electrode was washed with osmosis water. A cumulative release curve for fluoride (μg/cm^2), as a function of time was obtained for each experimental resin-based materials tested in this study.

For the analysis of Ca release up to 30 days (0, 1d, 3d, 7d, 14d, 21d, 30d), an absorbance photometry, turbidimetry, ion selective electrode technology was employed for the assessment of calcium release from the experimental composites over time (Spinreact Spin200E, Spinreact SAU, Esteve d'en Bas Girona, Spain). The reagents used were Phosphorus-UV (quantitative determination) and Calcium-A III (quantitative determination). A specific protocol, as per the manufacturer's (Spinreact) instructions, was employed for the determination of the calcium released in the media. It was performed at a wavelength of 650 nm using a cuvette with a light path length of 1 cm. The detection limit of the method was 0.26 μg/mL.

The assessment of phosphate (PO) release was conducted in accordance with the manufacturer's recommendations (Spinreact). Measurements were taken at a wavelength of 340 nm using a cuvette with a 1 cm light path. The detection limit of the method was 0.00 μg/mL. However, this method detected the presence of phosphorus unbound to organic molecules, usually as an orthophosphate molecule. Such a molecule reacts directly with the colourimetry reagent and the result

obtained was proportional to the concentration of phosphorus present in the specimens. In order to transform the equivalent value into phosphate, it was multiplied by the coefficient 3.06, which the results of the ration between the molecular weight of phosphate and the atomic weight of phosphorus. Finally, cumulative release curves for Ca and PO ($\mu g/cm^2$) as a function of time were obtained also in this case for each type tested material.

To determine statistically significant differences between the tested experimental groups, data analysis was conducted using Mann-Whitney tests. Post-hoc multiple comparisons were performed employing Bonferroni's correction for significance. The confidence level was set at 95 %. All statistical analyses were performed using IBM SPSS Statistics, Version 28.0 (Armonk, New York, NY, USA).

2.2. Surface analysis through FTIR-ATR and FIB-SEM/EDX

Sixteen specimens were prepared for each tested experimental resin-based materials (CTR, VS10-5 %; VS10-10 %; VS10-20 %; VS20-5 %; VS20-10 %; VS20-20 %) as described above, and randomly divided in 4 groups ($n = 4$/group) based on the different periods of immersion in simulated body fluid (SBF) over a period of 30 days (T0, 7d, 15d, 30d). The SBF was prepared as described by Kokubo et al. [24] by mixing NaCl (7.996 g), $NaHCO_3$ (0.350 g), KCl (0.224 g), $K_2HPO_3 \cdot 3H_2O$ (0.228 g), $MgCl_2 \cdot 6H_2O$ (0.305 g), $CaCl_2{\cdot}2H_2O$ (0.368 g), $NaSO_4$ (0.071 g), and 6.057 g $(CH_2OH)_3CNH_2$ (Tris buffer) per litre of SBF in distilled water. The pH was regulated at 7.0 using 1 N HCl.

The specimens were left undisturbed at 37 °C in SBF, which was replaced every 3 days, and analysed after different periods of immersion, as aforementioned. These were submitted to vibrational analysis in triplicate and the spectra were recorded in the range 3000–500 cm^{-1} with 32 scans at 4 cm^{-1} resolution using the Fourier-transform infrared (FTIR) spectrometer equipped with attenuated total reflection (ATR) device (Spectrum Two, Perkin Elmer, Madrid, Spain). The peaks were analysed subsequent to baseline subtraction and normalisation using the Spectrum 10™ software (Perkin Elmer) in order to identify the most characteristic inorganic compounds in the specimens.

Subsequent each FTIR analysis, the specimens from each group were mounted on stubs, gold-coated (MED 010, Balzers, Balzer, Liechtenstein), and finally observed through a an ultra-high-resolution analytical focused ion beam scanning electron microscope (FIB-SEM, Thermo Scientific Scios 2 DualBeam, Waltham, MA, USA) in secondary electron mode. The FIB-SEM was equipped with an energy dispersion-type x-ray spectroscope (EDX), which was used at 20 kV. During the EDX analysis, the specimens were assessed in six different areas in order to calculate the Ca/P ratio of the crystals.

2.3. High-performance liquid chromatography (HPLC) analysis

Five specimens were prepared for each experimental resin-based material following the outlined procedure. These specimens were submerged in 5 mL Eppendorf tubes filled with absolute ethanol and left undisturbed for 24 h at a constant temperature of 37 °C. Subsequently, a 0.5 mL aliquot of the storage solution was collected from each specimen and carefully transferred into an HPLC vial for further analysis.

The High-Performance Liquid Chromatography (HPLC) analysis was conducted using a system consisting of a quaternary pump (Waters 1525), an automated injector equipped with a 50 μL sample loop (Waters 2998 Plus), and a UV/VIS diode-array detector (Waters 2707). The specimens were injected "on-column" using a needle that was previously rinsed using 50 % acetonitrile in water. The chromatographic separation process was conducted at a controlled room temperature of 25 ± 2 °C, employing a C18 HPLC (150×4.6 mm) reverse-phase column packed with 5 μm silica particles (LiquidPurple, Analisis Vinicos, Tomelloso, Spain). The mobile phase used for the separation consisted of a mixture of acetonitrile and high-grade water (Merck Life Science, Madrid, Spain) in a ratio of 85:15 (v/v) [25,26].

The flow rate was adjusted to 1.0 mL/min, and UV detection at 215 nm. For the identified compounds, the retention times were 2.5 min for UDMA, 3.95 min for EDA, and 5.35 min for Bis-EMA. The methodology employed for the HPLC analysis was developed based on a modified approach outlined in previously published literature [25–27] and by emulating the parameters stipulated within the SIELC algorithm (SIELC© Technologies).

Standard solutions of UDMA, HEDA, and Bis-EMA were meticulously prepared in absolute ethanol, each at a concentration of 100 μg/mL for every monomeric compound. To establish the calibration curve, six distinct standard solutions were created, spanning concentrations of 0.5, 1, 5, 10, 50, and 100 μg/mL. Rigorous validation procedures were undertaken, demonstrating a high level of linearity ($R > 0.999$) for every monomeric compound within a concentration range of 0.5–100 μg/mL. The assumptions of normality and homogeneity of variances were considered in all of the analyses. Independent samples Student's *t*-tests [29] were performed to compare the mean values of VS10 and VS20 materials at each concentration and for each investigated monomer. Moreover, a repeated measures analysis of variance (ANOVA) was performed to assess the differences in monomers release. Post hoc Tukey's tests were conducted with a Bonferroni correction to account for multiple comparisons ($\alpha = 0.05$). All statistical analyses were carried out using IBM SPSS Statistics, Version 28.0. (Armonk, New York, NY, USA).

2.4. Evaluation of bacterial metabolic activity and viability

Five specimens were prepared for each tested experimental composite as described above, polished for 30 s under irrigation (distilled water) using a 1200 SiC-grit paper and finally rinsed with Milli-Q water. The specimens were immersed in 25 mL of sterile PBS in 50 mL polypropylene tubes for 48 h at room temperature. Previous to exposure to bacteria, the specimens were removed from PBS and rinsed again with Milli-Q water and sterilised via UV-light (10 min per side).

S. gordonii, a Gram+ primary coloniser of oral and dental surfaces, was used to evaluate the antibacterial ability of the experimental composites tested in this study [28]. Bacteria were obtained from Type Culture Collection (804 CECT, Spain). *S. gordonii* inoculum was obtained by culturing bacteria in Tryptic Soy Broth (TSB, Bacto BD, Germany) overnight at 37 °C and 150 rpm. For each experiment, the bacteria concentration was adjusted to an optical density (O.D.) at 600 nm; then a double 1:10 dilution was performed, and 200 μL of the 1:100 bacteria suspension was added to each tested sample in a 48 well-plate and incubated for 24 h at 37 °C and 150 rpm.

Metabolic activity was evaluated after 24 h using Adenosine triphosphate (ATP) bioluminescent (BacTiter-Glo, Promega, USA). The specimens were transferred to new 48 well-plate and incubated in 400 μL of a 50:50 solution of PBS:ATP for 5 min at 37 °C and protected from light. 200 μL of the solution was then transferred to a white flat bottom 96 well-plate and luminescence measurement was performed in a microplate reader (Synergy HT, Biotek, USA).

Colony Forming Units (CFU) counting was also performed to assess the viability of *S. gordonii* on the surface of the tested materials and to corroborate the antimicrobial ability obtained with the ATP test. After 24 h incubation, five more specimens per group prepared as described above and transferred into Eppendorf containers containing 1 mL of sterile Dulbecco's Phosphate Buffered Saline (DPBS, D8537 Merk, Spain). For the detection of the bacteria the specimens were vortexed for 5 min and sonicated for 1 min. Serial dilutions were performed in DPBS. A 5 μL sample was obtained from each dilution (triplicates) and cultured on brain heart infusion-agar plates (CM 1136, OXOID) for 48 h at 37 °C, and finally colonies were counted.

Moreover, LIVE/DEAD stained bacteria visualization by confocal laser scanning was performed on three additional discs per group. The specimens were first washed with PBS and immersed in a solution containing an equimolar solution of propidium iodide (red staining) and Syto-9 (green staining) prepared in Ringer's, according to the

Table 1
Storage media - pH of the tested materials over a period of 30 days.

	0d	1d	3d	7d	15d	21d	30d
CTR	6.18 ± 0.05	6.33 ± 0.16	6.19 ± 0.01	6.23 ± 0.02	6.25 ± 0.02	6.13 ± 0.08	6.33 ± 0.01
VS10-5 %	6.13 ± 0.01	6.33 ± 0.03	6.35 ± 0.02	6.51 ± 0.01	6.35 ± 0.01	6.37 ± 0.05	6.31 ± 0.03
VS10-10 %	6.13 ± 0.01	6.32 ± 0.01	6.35 ± 0.07	6.50 ± 0.01	6.35 ± 0.01	6.35 ± 0.01	6.29 ± 0.01
VS10-20 %	6.15 ± 0.02	6.31 ± 0.01	6.35 ± 0.01	6.38 ± 0.01	6.37 ± 0.05	6.35 ± 0.01	6.29 ± 0.01
VS20-5 %	6.15 ± 0.02	6.13 ± 0.01	6.35 ± 0.10	6.22 ± 0.10	6.21 ± 0.02	6.21 ± 0.03	6.35 ± 0.01
VS20-10 %	6.23 ± 0.01	6.13 ± 0.01	6.15 ± 0.01	6.16 ± 0.03	6.16 ± 0.02	6.23 ± 0.01	6.35 ± 0.01
VS20-20 %	6.19 ± 0.01	6.19 ± 0.11	6.15 ± 0.01	6.15 ± 0.05	6.25 ± 0.02	6.32 ± 0.10	6.31 ± 0.01

manufacturer instructions (LIVE/DEAD™, Invitrogen L7012). Images were obtained using a fluorescence confocal microscope (Leica SP8, Germany) and analysed in the LAS X software (Leica) to observe the intact membrane bacteria cells (green fluorescence) and the compromised membranes of cells (red fluorescence).

Mean and standard deviation values were calculated, and the results were firstly analysed by Levene's tests to assess homogeneity of variances between groups. ANOVA, along with Tukey and Tamahane's T2 post-hoc multiple comparison tests were performed for ATP and CFU, respectively ($p < 0.05$).

3. Results

3.1. pH and ions release evaluation

The mean and standard deviations (±SD) values of the pH of the storage media of all the tested materials over a period of 30 days are shown in Table 1. No particular change in pH was observed over time, as all the tested materials showed values between 6.1 and 6.4

Regarding the release of fluoride ions, mean and standard deviation (±SD) values are depicted in μg/cm^2 in Table 2. Overall, The tested composites containing the FDCP filler VS20 showed higher release of fluoride ions ($p < 0.05$) at all different time of measurements compared to those composites containing the VS10 filler. The composite with the highest fluoride ions release was VS20-20 % from day 7 (571.3 ± 49.5 μg/cm^2), with a fluoride concentration that remained constant (49.4 ± 4.6 μg/cm^2) from day 14 up to day 30.

It was possible to observe that the all the experimental composites containing the FDCP filler VS10 had their maximum release of fluoride between 7 and 14 days of storage ($p < 0.05$), while those containing the filler VS20 had their maximum fluoride release between day 3 and 7 ($p < 0.05$). The tested composites containing VS20 started releasing a significant ($p < 0.05$) amount of fluoride ions at the day 1 only, which was significantly greater ($p < 0.05$) compared to those composites containing the FDCP filler VS10. Moreover, such a release of fluoride from the experimental composites containing the filler VS20 at day 1 was significantly higher ($p < 0.05$) with increased concentration of the filler (VS20-20 % > VS20-10 % > VS20-5 %). Conversely, the release of fluoride from the experimental composites containing VS10 at day 1, 3 and 7 showed no significant increase ($p > 0.05$), with higher concentration of the filler (VS10-20 % = VS10-10 % = VS10-5 %). The experimental composites containing the FDCP filler VS10 that presented the highest release of fluoride ($p < 0.05$) was that containing a concentration of 20 %; this occurred at day 14. All the tested materials at day 21 reached a plateau in fluoride release without any significant ($p > 0.05$) change up to 30 days.

The results of Ca ions release (μg/cm^2) from the tested materials are depicted in Table 3 as mean and standard deviation (±SD) values. Overall, the experimental composites containing the FDCP filler VS10 showed higher release of Ca ($p < 0.05$) at all different times compared to those composites containing the VS20 filler. All the composites containing the FDCP filler VS10 had their maximum release of Ca ions between day 14 and 30 ($p < 0.05$), as well as those containing the VS20, although these latter were significantly lower in comparison to those with the FDCP filler VS10 ($p < 0.05$); the only exception was VS20-20 % that showed comparable ($p > 0.05$) Ca release to VS10-20 % at day 14 (19.1 ± 6.1 and 20.5 ± 2.1, respectively). However, all composites containing VS10 started accumulated a significant ($p < 0.05$) amount of Ca at the day 1 only, while only VS20-10 % and VS20-20 % had the same behaviour, but in a significant lower amount ($p < 0.05$) compared to those composites containing VS10. Such a release of Ca from the experimental composites containing VS20 was significantly higher ($p < 0.05$) only with a concentration of the filler of 20 %. Conversely, the composites containing VS10 showed significant ($p < 0.05$) higher amount of Ca release at increased concentration at day 3 (VS10-20 % = VS10-10 % > VS10-5 %). At day 14, the composite VS10-20 % had the greatest release of Ca ($p > 0.05$), (VS10-20 % > VS10-10 % = VS10-5 %), but from day 21, all the concentrations of VS10 presented no difference ($p > 0.05$) in Ca release (VS10-20 % = VS10-10 % = VS10-5 %).

The results of phosphate (PO) ions release (μg/cm^2) from the tested materials are depicted as mean and standard deviation (±SD) values in Table 4. In this case, all the experimental composites containing the

Table 2
Release of fluoride ions from the tested material over a period of 30 days.

Time (Day)	CTR	VS10-5 %	VS20-5 %	VS10-10 %	VS20-10 %	VS10-20 %	VS20-20 %
0	0.04 ± 0.11^{Aa1}	$0.01 \pm 0.00^{A1*}$	$0.68 \pm 0.39^{b1£}$	$0.00 \pm 0.00^{A1*}$	$2.81 \pm 1.58^{c1£}$	$0.00 \pm 0.00^{A1*}$	$4.65 \pm 3.33^{c1£}$
1	0.04 ± 0.14^{Aa1}	$0.01 \pm 0.00^{A1*}$	$22.08 \pm 8.00^{b2£}$	$0.00 \pm 0.01^{A1*}$	$41.64 \pm 8.84^{c2£}$	$0.01 \pm 0.01^{A1*}$	$50.35 \pm 4.27^{c2£}$
3	0.08 ± 0.10^{Aa1}	$1.08 \pm 0.27^{B2*}$	$124.55 \pm 14.88^{b3£}$	$1.36 \pm 0.24^{B2*}$	$309.02 \pm 40.07^{c3£}$	$1.82 \pm 0.18^{B2*}$	$297.89 \pm 74.88^{c3£}$
7	0.04 ± 0.14^{Aa1}	$5.43 \pm 0.78^{B3*}$	$159.76 \pm 62.08^{b3£}$	$5.70 \pm 1.21^{B3*}$	$283.93 \pm 87.73^{b3£}$	$6.69 \pm 0.19^{B3*}$	$571.36 \pm 49.52^{c4£}$
15	0.05 ± 0.15^{Aa1}	$3.87 \pm 0.57^{B4*}$	$14.42 \pm 2.39^{b4£}$	$4.02 \pm 0.93^{B3*}$	$29.73 \pm 6.20^{c4£}$	$13.79 \pm 1.13^{C4*}$	$43.37 \pm 5.48^{d2£}$
21	0.07 ± 0.09^{Aa1}	$1.04 \pm 2.06^{B2*}$	$14.26 \pm 2.45^{b4£}$	$1.41 \pm 0.15^{B2*}$	$29.48 \pm 6.23^{c4£}$	$1.12 \pm 0.65^{B2*}$	43.11 ± 5.55^{d23}
30	0.08 ± 0.18^{Aa1}	$1.02 \pm 0.49^{B2*}$	$17.61 \pm 1.87^{b4£}$	$1.15 \pm 0.06^{B2*}$	$31.28 \pm 6.38^{c4£}$	$1.07 \pm 0.06^{B2*}$	$49.38 \pm 4.57^{d2£}$

Values are depicted as mean and standard deviation (±SD) in μg/cm^2
(A.B.C.D) Different uppercase letters indicate significance in rows between the results obtained with composites having the same filler (VS 10) at different concentration (CTR, R5 to R20) at the same time.
(a.b.c) Different uppercase letters indicate significance in rows between the results obtained with composites having the same filler (VS 20) at different concentration (CTR, R5 to R20) at the same time.
(1,2,3) Different numbers indicate significance in columns between the results obtained with composites having the same filler (CTR - VS10 - VS20) at same concentration but at different time (0 to 30 days).
(*,£) Different symbol indicates significance in row between the results obtained with composites having different filler (VS10 or VS20) at same concentration and time.

Table 3
Release of calcium ions from the tested material over a period of 30 days.

Time (Day)	CTR	VS10-5 %	VS20-5 %	VS10-10 %	VS20-10 %	VS10-20 %	VS20-20 %
0	0.00 ± 0.00^{Aa1}	$0.0 \pm 0.00^{A1*}$	$0.00 \pm 0.00^{a1*}$	$0.00 \pm 0.00^{A1*}$	$0.00 \pm 0.00^{a1*}$	$0.00 \pm 0.00^{A1*}$	$0.00 \pm 0.00^{a1*}$
1	0.00 ± 0.00^{Aa1}	$2.63 \pm 0.83^{B2*}$	$0.00 \pm 0.00^{a1£}$	$7.66 \pm 2.10^{C2*}$	$0.22 \pm 0.54^{a1£}$	$8.75 \pm 2.44^{C2*}$	$1.05 \pm 4.29^{a1£}$
3	0.00 ± 0.00^{Aa1}	$3.63 \pm 1.80^{B2*}$	$0.00 \pm 0.00^{a1£}$	$7.77 \pm 0.78^{C2*}$	$0.35 \pm 1.10^{a1£}$	$9.82 \pm 3.68^{C2*}$	$1.10 \pm 3.42^{b1£}$
7	0.00 ± 0.00^{Aa1}	$6.20 \pm 2.23^{B3*}$	$0.00 \pm 0.00^{a1£}$	$8.96 \pm 0.65^{B2*}$	$1.56 \pm 1.77^{a1£}$	$17.33 \pm 6.85^{C3*}$	$1.15 \pm 0.36^{a1£}$
15	0.00 ± 0.00^{Aa1}	$10.85 \pm 5.46^{B4*}$	$9.19 \pm 1.86^{b2£}$	$9.15 \pm 1.09^{B2*}$	$12.14 \pm 1.57^{b2*}$	$19.18 \pm 6.12^{C4*}$	$20.55 \pm 2.17^{c2*}$
21	0.00 ± 0.00^{Aa1}	$40.44 \pm 6.04^{B5*}$	$9.63 \pm 1.88^{b2£}$	$44.97 \pm 5.19^{B3*}$	$10.96 \pm 1.00^{b2£}$	$46.27 \pm 4.23^{B5*}$	$15.41 \pm 0.93^{c3£}$
30	0.00 ± 0.00^{Aa1}	$39.59 \pm 4.57^{B5*}$	$9.19 \pm 1.70^{b2£}$	$44.85 \pm 5.53^{B3*}$	$11.09 \pm 1.01^{b2£}$	$49.90 \pm 3.19^{B5*}$	$14.49 \pm 1.05^{b3£}$

Values are depicted as mean and standard deviation (±SD) in μg/cm^2.
$^{(A.B.C.D)}$ Different uppercase letters indicate significance in rows between the results obtained with composites having the same filler (VS 10) at different concentration (CTR, R5 to R20) at the same time.
$^{(a.b.c)}$ Different uppercase letters indicate significance in rows between the results obtained with composites having the same filler (VS 20) at different concentration (CTR, R5 to R20) at the same time.
$^{(1,2,3)}$ Different numbers indicate significance in columns between the results obtained with composites having the same filler (CTR - VS10 - VS20) at same concentration but at different time (0 to 30 days).
$^{(*,£)}$ Different symbol indicates significance in row between the results obtained with composites having different filler (VS10 or VS20) at same concentration and time.

FDCP filler VS10 or VS20 started releasing a significant ($p < 0.05$) amount of PO ions at the day 1, excluding VS10-5 % and VS10-5 %; these values remained constant ($p > 0.05$) up to day 14 and reached the maxim PO release values at day 21; no more change was observed up to day 30. The composite VS10-5 % showed a significant ($p < 0.05$) lower PO compared to VS20-5 % only at day 14. VS10-10 % showed a significant ($p < 0.05$) lower release of PO compared to VS20-10 % only at day 14, while they had a similar release of PO at day 7. The composite VS10-20 % showed a significant ($p < 0.05$) lower PO releasing compared to VS20-20 % only at day 1 and 3.

The release of PO from the experimental composite containing the FDCP filler VS20 was significantly higher ($p < 0.05$) at high concentration of such a FDCP filler (VS20-20 % > VS20-10 %) from day 3. The composite containing the FDCP filler VS10 presented significantly higher ($p < 0.05$) PO release at high concentration of such a FDCP filler (VS10-20 % > VS10-10 % > VS10-5 %) from day 1. However, the composite with the higher PO release were VS10-20 % from day 1 and VS20-20 % from day 3.

3.2. Surface analysis through FTIR-ATR

The FTIR-ATR results obtained at baseline on the surface of the tested materials are presented in Fig. 1. In details, the control (CTR: no FDCP filler) composite containing no FDCP filler (A) had characteristic absorption peaks such as organic methacrylate monomers (1720 cm^{-1}, 1640 cm^{-1}, and 1454 cm^{-1}). Moreover, C–H stretch at 2950–2850 cm^{-1}, C=O stretch at 1720 cm^{-1}, the aliphatic C=C at 1640 cm^{-1} and the aromatic C=C at 1610 cm^{-1} were also observed. The N–H bend of UDMA was detected at 1520 cm^{-1}, while the C–O stretch of Bis-EMA and UDMA were observed at 1240 cm^{-1} and 1320 cm^{-1}. It was also possible to detect the C–O–C groups in HEDA (1115 cm^{-1}), as well as the C–O–C, and the C–C–O stretch (940 cm^{-1} and 830 cm^{-1}, respectively). The symmetric Si–O stretch of the glass filler was seen at 790 cm^{-1} On the other hand, all the experimental resins containing the FDCP fillers, such as VS10-5 % (Fig. 1B), VS10-10 % (Fig. 1C), VS20-20 % (Fig. 1D), presented the same peaks as the CTR composite, but with the presence of a further peak at 1136 cm^{-1} associated to the stretching modes of the pyrophosphate ($P_2O_7^{4-}$).

The FTIR-ATR results after 15 days of SBF storage demonstrated that CTR composite (Fig. 1E) presented a comparable spectra to that observed at the baseline. Conversely, VS10-5 % (Fig. 1F) after 15-day SBF, VS10-10 % (Fig. 1G) after 7-day SBF and VS10-20 % (Fig. 1H) after 15-day SBF showed all the PO stretching of apatite peaks (559 cm^{-1}, 600 cm^{-1}, 962 cm^{-1}, 1021 cm^{-1}). Other phosphate bands assigned to the phosphate group ($\nu 3$) were also detected (1088 cm^{-1} and 1036 cm^{-1}). The absence of any strong absorbance peak at 1400–1600 cm^{-1} and at about 875 cm^{-1} suggests that no carbonate group was present in any of the tested experimental materials after storage in SBF. Peaks observed at around 1128 cm^{-1} and 1070 cm^{-1} were due to symmetric P-O stretching vibration of PO_3^{2-}.

Regarding the experimental composite containing VS20, no peaks of apatite were seen in VS20-5 % (Fig. 1I) after 15 days of SFB storage; this material (Fig. 1L)) required 30 days to show a clear formation of apatite. The experimental composite containing VS20-10 % (Fig. 1M) was the only one to produce apatite after 7 days of SFB storage. Conversely, VS20-20 % (Fig. 1N)) showed a peaks of apatite after 15 days of SBF storage.

Table 4
Release of phosphate ions from the tested material over a period of 30 days.

Time (Day)	CTR	VS10-5 %	VS20-5 %	VS10-10 %	VS20-10 %	VS10-20 %	VS20-20 %
0	0.00 ± 0.00^{Aa1}	$0.00 \pm 0.00^{A1*}$	$0.00 \pm 0.00^{a1*}$	$0.00 \pm 0.00^{A1*}$	$0.00 \pm 0.00^{a1*}$	$0.00 \pm 0.00^{A1*}$	$0.00 \pm 0.00^{a1*}$
1	0.00 ± 0.00^{Aa1}	$0.61 \pm 1.12^{A1*}$	$0.90 \pm 1.20A^{a2*}$	$3.36 \pm 2.08^{B2*}$	$2.01 \pm 2.20^{b2*}$	$7.37 \pm 2.08^{C2*}$	2.68 ± 2.08^{b2}
3	0.00 ± 0.00^{Aa1}	$0.57 \pm 1.65^{A1*}$	$1.43 \pm 2.08^{b2*}$	$4.27 \pm 2.48^{B2*}$	$5.45 \pm 2.14^{c3*}$	$10.83 \pm 1.59^{C3*}$	$6.48 \pm 2.11^{c3£}$
7	0.00 ± 0.00^{Aa1}	$1.37 \pm 2.05^{B2*}$	$1.26 \pm 1.53^{b2*}$	$7.87 \pm 2.26^{C3*}$	$8.18 \pm 2.42^{c3*}$	$13.71 \pm 1.62^{D3*}$	$14.44 \pm 2.36^{d4*}$
15	0.00 ± 0.00^{Aa1}	$1.43 \pm 2.14^{B2*}$	$6.52 \pm 1.53^{b3£}$	$8.77 \pm 0.18^{C3*}$	$15.48 \pm 3.40^{c4£}$	$14.98 \pm 2.11^{D3*}$	$16.16 \pm 4.41^{C4*}$
21	0.00 ± 0.00^{Aa1}	$4.18 \pm 0.18^{B3*}$	$5.20 \pm 1.59^{c3*}$	$11.16 \pm 2.23^{C4*}$	$12.34 \pm 3.52^{d4*}$	$17.63 \pm 3.00^{D4*}$	$15.34 \pm 0.43^{d4*}$
30	0.00 ± 0.00^{Aa1}	$4.37 \pm 0.18^{B3*}$	$5.07 \pm 2.11^{B3*}$	$11.97 \pm 1.77^{C4*}$	$11.51 \pm 4.50^{c4*}$	$17.68 \pm 1.68^{D4*}$	$15.58 \pm 2.33^{C4*}$

Values are depicted as mean and standard deviation (±SD) in μg/cm^2.
$^{(A.B.C.D)}$ Different uppercase letters indicate significance in rows between the results obtained with composites having the same filler (VS 10) at different concentration (CTR, R5 to R20) at the same time.
$^{(a.b.c)}$ Different uppercase letters indicate significance in rows between the results obtained with composites having the same filler (VS 20) at different concentration (CTR, R5 to R20) at the same time.
$^{(1,2,3)}$ Different numbers indicate significance in columns between the results obtained with composites having the same filler (CTR - VS10 - VS20) at same concentration but at different time (0 to 30 days).
$^{(*,£)}$ Different symbol indicates significance in row between the results obtained with composites having different filler (VS10 or VS20) at same concentration and time.

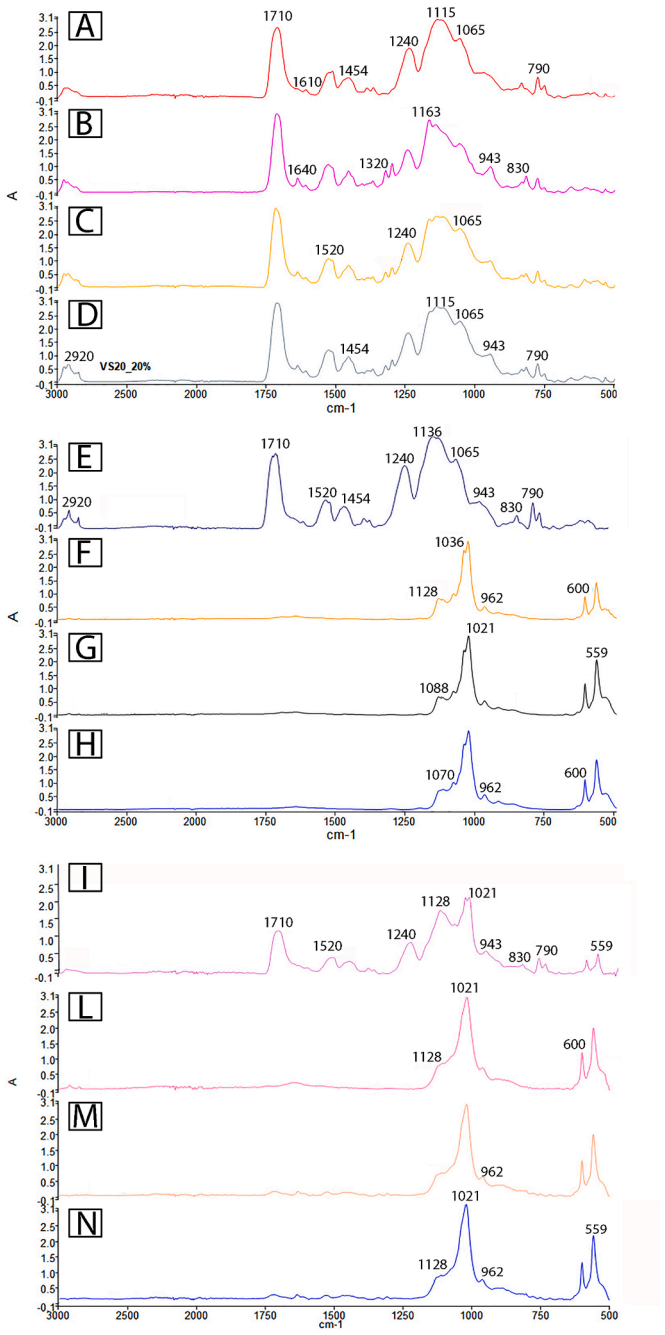

Fig. 1. Infrared spectra of reference and experimental composites with FCDC filler. (A) Spectrum of the control composite without FCDC filler at baseline, showing characteristic peaks of organic methacrylate monomers. (B) VS10-5 %, (C) VS10-10 %, (D) VS20-20 %, with the additional peak at 1136 cm^{-1} associated with the stretching modes of the pyrophosphate anion ($P_2O_7^{4-}$). (E) Control composite without FCDC filler after 30 days in simulated body fluid (SBF), exhibiting spectra similar to baseline. (F) VS10-5 % after 15 days, (G) VS10-10 % after 7 days, and (H) VS10-20 % after 15 days of SBF storage, showing all the PO stretching peaks of hydroxyapatite. (I) VS20-5 % without apatite formation after 15 days in SBF, while (L) VS20-5 % displays clear apatite formation on the surface after 30 days. The only material to exhibit clear PO stretching peaks of hydroxyapatite after 7 days is the composite (M) VS20-10 %, whereas composite (N) VS20-20 % requires 15 days of SBF storage to show a distinct formation of apatite on the surface.

3.3. Crystallographic surface assessment through FIB-SEM/EDX

The SEM micrographs and EDX spectra of the specimens tested at baseline are presented in Fig. 2, while those for Ca/P ratio are depicted in Table 5. Important features were observed in this part of the study. For instance, the flat surfaces of the specimens created with the control composite (CTR) were devoid of any presence of mineral crystals also when imaged at higher magnification (Fig. 2A and A1); only the presence of Si from the glass filler was detected during the EDX analysis (Fig. 2A2) and the Ca/P ratio confirmed the absence of any deposition of calcium phosphate (Table 5). Conversely, although the experimental composite containing the VS10 filler (VS10-10 %) presented a flat surface with no mineral crystals (Fig. 2B and B1). These latter specimens showed an EDX spectra characterised by the presence of Si from the glass filler, along with Ca and P from the FDCP filler and a very low presence of fluoride (Fig. 2B2). In this case, the Ca/P ratio for the composites VS10-5 %, VS10-10 % and VS10-20 % was 26.1, 36.8 and 28.8, respectively. The situation was similar for the composite containing the FDCP filler VS20, which showed no crystals (Fig. 2C and C1) and the presence of Si, Ca and P, along with a low signal of fluoride (Fig. 2C2). In this case, the Ca/P ratio for the was the VS20-5 % and VS20-10 % was 33.4 and 35.2, respectively. The VS20-20 % presented similar morphological results (Fig. 2D and D1) and a Ca/P ration of 34.5.

The SEM micrographs and EDX spectra of the control composite and those containing the filler VS10 after SBF storage are presented in Fig. 3. The composite containing no FDCP (CTR) presented after 30 days of storage in SBF a rough surface without any deposition of mineral crystals (Fig. 3A and A1). The EDX analysis performed on these latter specimens showed the traces of Ca, P, Na, K, Mg and Cl, which were probably absorbed during prolonged SBF storage (Fig. 3A2). The Ca/P ratio for this composite at 7d, 15d and 30 days was 0.77, 2.74 and 3.07, respectively. Conversely, all the composites containing the FDCP filler VS10, presented their surfaces completely covered by plate-like crystals (Fig. 3B and B1) after 15 days of SBF, excluding the VS10-10 % that was the only composite to show a surface totally covered by crystals (Fig. 3C and C1) after 7 days of SBF. The EDX spectra was characterised by a prominent presence of Ca and P from the new crystals formed on the composite's surface, along with Na, Mg and Cl; almost no fluoride was detected (Fig. 3B2). The Ca/P ratio of the composites containing the FDCP VS10 at 7d, 15d and 30 days was in a range between 1.33 and 1.35. Also in this case, the specimens were rich in Ca and P, along with the presence of Na, Mg and Cl, and a very low presence of fluoride (Fig. 3C2). The experimental VS10-20 % only after 15 days of SBF storage (Fig. 3D and D1) had a fully crystallisation of the surface (Fig. 3C2). In this case the Ca/P ratio at 7d, 15d and 30 days was between 1.33 and 1.34.

The specimens created with the experimental composite VS20-10 % evoked a full surface after 7 days of SBF storage (Fig. 4C and C1), with an EDX spectra characterised by an abundant presence of Ca and P, along with low presence of Na, Mg and Cl, and very low fluoride (Fig. 4C2). The Ca/P ratio composites containing the FDCP filler VS20 at 7d, 15d and 30 days was in a range between 1.33 and 1.35, respectively. The composite VS20-20 % obtained the same morphological features (Fig. 4D and D1) and Ca/P ratio (Fig. 4D2) as the VS20-10 %, but only after 15 days of SBF storage.

3.4. High-performance liquid chromatography (HPLC)

The results for the elution (μg/mL) of UDMA, BisEMA and HEDA from the tested materials at 24 h are depicted in Table 6 as mean and standard deviation (±SD) values. In terms of UDMA elution, all the experimental composites containing the FDCP filler VS20 showed significant higher values ($p < 0.05$) compared to those composites containing VS10. These latter resins exhibited values similar to those of the control FDCP-free composite ($p > 0.05$), except for the VS10-5 % that showed the lowest UDMA elution over a period of 24 h ($p < 0.05$). The

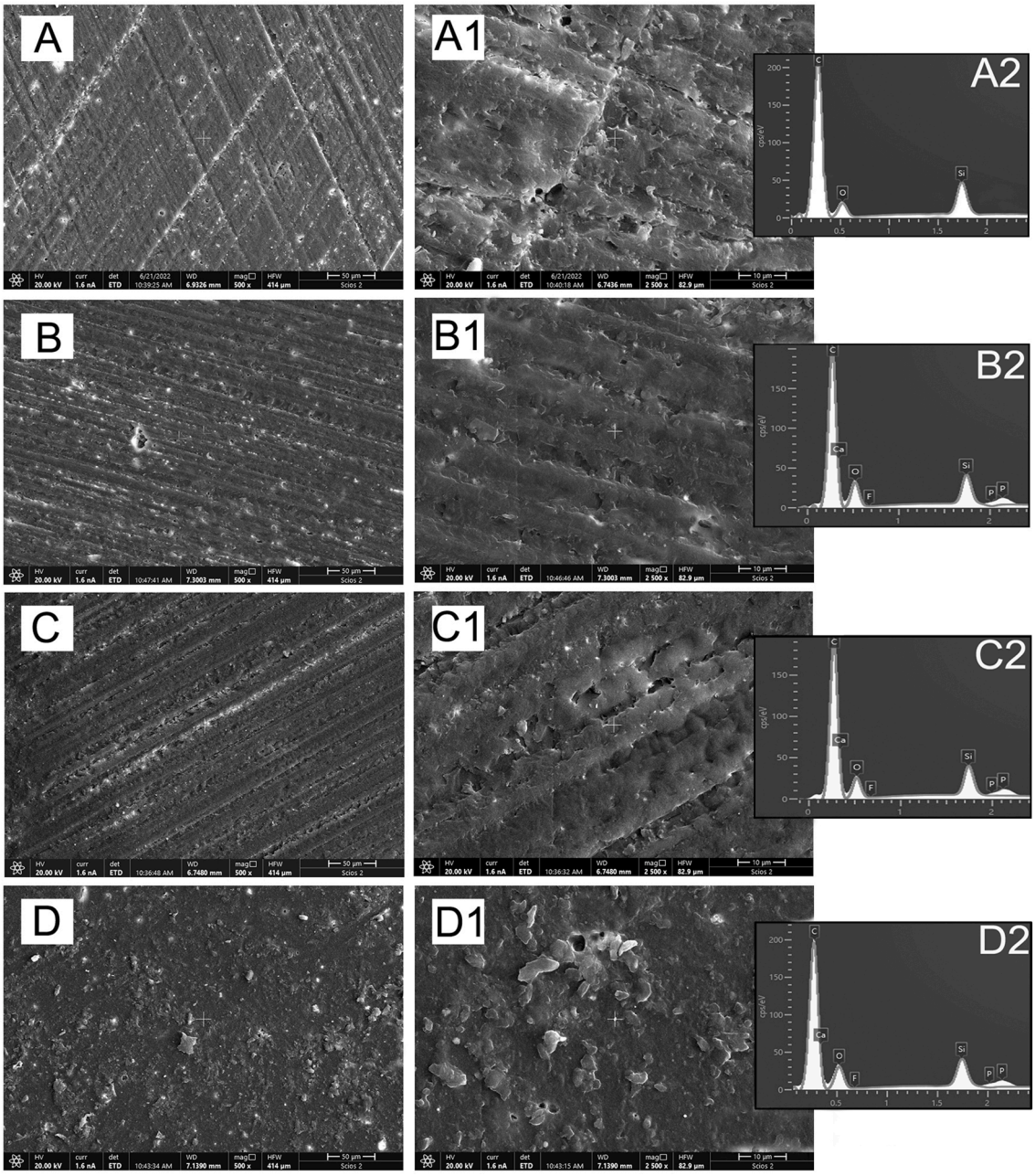

Fig. 2. A: Representative SEM micrograph of the composite control containing no FDCP showing a flat surface devoid of any presence of mineral crystals also at higher magnification (A1). The EDX analysis highlights the presence of Si from the glass filler, but no Ca and P (A2). B: Representative SEM micrograph of the experimental composite containing 10 % of the FDCP filler VS10 (VS10-10 %) showing a flat surface devoid of any presence of mineral crystals also at higher magnification (B1). In this case it possible to observe in the EDX spectra the presence of Si from the glass filler and Ca and P from the FDCP filler; the signa for fluoride is very low (B2). C: Representative SEM micrograph of the experimental composite containing 10 % of the FDCP filler VS20 (VS20-10 %) showing a flat surface devoid of any presence of mineral crystals also at higher magnification (C1). Also in this case it possible to observe in the EDX spectra the presence of Si from the glass filler and Ca and P from the FDCP filler; the signa for fluoride is very low (C2). D: Representative SEM micrograph of the experimental composite containing 20 % of the FDCP filler VS20 (VS20-20 %) with no presence of mineral crystals at higher magnification (D1). Also in this case it possible to observe in the EDX spectra the presence of Si from the glass filler and Ca and P from the FDCP filler. Although in this resin there is high concentration of FDCP, the signal for fluoride is still very low (C2).

same trend was observed in terms of BisEMA release, since the experimental composites containing VS20 had significant higher values ($p < 0.05$) compared to the composites containing VS10. In terms of HEDA elution, although the experimental composites containing VS20 had significant higher values ($p < 0.05$) compared to those containing VS10, they had a significant lower elution of HEDA compared to the control FDCP-free composite ($p < 0.05$).

3.5. Bacterial deposition, metabolic activity and viability of S. gordonii

The results of ATP bioluminscence of *S. gordonii* cultured on the surface of the different materials tested in this study are illustrated in Fig. 5. All resins containing the FDCP fillers significantly reduced bacterial vitality ($p < 0.05$) compared to the control FDCP-free resin. Notably, the experimental composites containing VS10 or VS20 at a concentration of 10 % induced the lowest bacterial ATP activity,

Table 5
CaP ratio of the tested material over a period of 0, 15 and 30 days of SBF storge.

	T0 - baseline			7d			15d			30d		
	Ca wt%	P wt%	**Ca/P**	Ca wt%	P wt%	**Ca/P**	Ca wt%	P wt%	**Ca/P**	Ca wt%	P wt%	**Ca/P**
CTR	0.00±0.0	0.0 ± 0.0	**0.00±0.00**	0.01±0.02	0.0 ± 0.001	**0.77±1.34**	1.50±0.32	0.40±0.12	**2.74±0.15**	1.63±0.43	0.40±0.06	**3.07±0.67**
VS10-5 %	0.44±0.12	0.01±0.01	**26.1 ± 9.8**	1.24±0.09	016±0.01	**6.13±0.23**	36.1 ± 0.74	20.8 ± 0.49	**1.34±0.06**	36.5 ± 0.46	21.2 ± 1.1	**1.33±0.09**
VS10-10 %	0.48±0.06	0.01±0.01	**36.8 ± 4.9**	36.3 ± 0.81	21.1 ± 0.21	**1.33±0.04**	35.5 ± 0.55	20.7 ± 0.56	**1.33±0.03**	35.5 ± 0.55	20.7 ± 0.56	**1.35±0.04**
VS10-20 %	1.83±0.44	0.05±0.01	**28.8 ± 7.4**	1.33±0.31	0.07±0.02	**5.96±0.42**	36.2 ± 1.51	21.0 ± 0.62	**1.33±0.02**	36.4 ± 1.15	20.9 ± 0.55	**1.34±0.05**
VS20-5 %	0.43±0.15	0.01±0.01	**33.4 ± 11.8**	1.00±0.10	0.31±0.07	**2.58±0.7**	2.60±1.48	0.35±0.15	**5.81±2.08**	35.7 ± 1.04	20.0 ± 1.13	**1.33±0.03**
VS20-10 %	0.46±0.05	0.02±0.01	**35.2 ± 3.89**	35.8 ± 0.52	20.6 ± 0.64	**1.33±0.06**	35.7 ± 0.40	20.7 ± 0.56	**1.33±0.05**	35.1 ± 1.0	20.3 ± 0.64	**1.35±0.04**
VS20-20 %	1.03±0.18	0.02±0.01	**34.5 ± 3.38**	1.7 ± 0.41	0.40±0.07	**4.26±0.23**	36.0 ± 1.08	21.1 ± 0.26	**1.32±0.03**	36.9 ± 0.2	21.4 ± 046	**1.33±0.02**

although with no statistical significance difference compared to all other FDPC-containing composites.

The results of the *S. gordonii* viability (CFU/mL) on the different tested materials are depicted in Fig. 6. CFU values for the different groups had analogous trends to those obtained for ATP activity. Indeed, the experimental composites containing 10 % of VS10 or VS20 had the lowest colony counting, with larger than one order of magnitude and significant difference ($p < 0.05$) compared to the control composite. All other composites containing the FDCP fillers reduced bacteria viability compared with FDCP-free control resin, but with no significant difference.

LIVE/DEAD images of *S. gordonii* grown after cultured on different tested materials are shown in Fig. 7. In details, it was possible to see that bacteria colonised the surface in all cases. However, similar trends to those for ATP and CFU results were observed, as composites SV10-R10 % and SV20-R10 % presented their surfaces colonised by less bacteria; a simple monolayer of cells was detected in these specimens. Conversely, the control surfaces presented a multilayer structure similar to that of SV10-R20 % and SV20-R20 %. However, from the ATP and CFU results it was clear that the bacteria vitality and even viability, was lower on the surfaces of the experimental composites containing the FDCP fillers. Of note, only a few red-stained dead bacteria were visualised on all tested specimens, which could be due to PBS cleaning that removed such dead bacteria from the surface.

4. Discussion

The remineralisation of mineral-depleted dental hard tissues may be achieved when employing dental biomaterials that can release specific ions such as fluoride (F), calcium (Ca) and phosphate (PO) ions that exceeds those present in the surrounding saliva [29,30]. The first effort of the present project was to develop a number of experimental resin-based composites containing different concentrations of fluoride-doped calcium phosphates (FDCP) fillers, and evaluate the cumulative amount of Ca, PO and F released at standard condition (pH) in deionised water up to a period of 30 days. The main outcome was that the pH of the solution remained stable during the entire period of assessment for F, Ca and PO accumulation (pH range: 6.12–6.37; Table 1). In this regard, the release of fluoride ions (μg/cm^2) since day 1 from the experimental composites containing the FDCP filler VS20 was higher compared to those composites containing VS10 (Table 2). The highest level of fluoride accumulated at day 7 (571.4 μg/cm^2) was achieved by the composite VS20-20 %; this latter showed no significant increase in F concentration from day 14 (43.4 μg/cm^2) up to day 30 (49.4 μg/cm^2). On the other hand, the experimental composites containing the FDCP filler VS10 that presented the highest ($p < 0.05$) release of fluoride was SV10-20 % (13.8 μg/cm^2). However, all the experimental composites had no significant ($p > 0.05$) accumulation of fluoride between 21 and 30 days at standard pH condition. Regarding the release of Ca (μg/cm^2), the experimental composites containing the VS10 filler showed overall higher ($p < 0.05$) values compared to those composites containing the VS20 filler (Table 3). These differences in fluoride release between the tested composites can be attributed to the different composition of the FDCP fillers employed in this study to formulate the experimental composites; VS20 contains more fluoride salts (CaF 10wt% and CaNa 10wt%) than the VS10 (CaF 5wt% and CaNa 5wt%) [22]. Moreover, the composites containing VS10 showed significant ($p < 0.05$) higher amount of Ca accumulation at increased FDCP concentration, especially at day 14 (VS10-20 % > VS10-10 % = VS10-5 %), but from day 21, all of them presented no difference ($p > 0.05$) in terms of Ca accumulation in the storage media (VS10-20 % = VS10-10 % = VS10-5 %). These latter outcomes indicate that a great part of the Ca released in the media may have reacted with other ions such as F and PO, which precipitated as a more complex calcium phosphate. Moreover, as well as in the case of F release, the tested materials were not able to release any further significant amount of Ca from day 21. Hence, further studies are already ongoing to investigate the Ca and F rechargeability of such experimental composites, as well as the maximum number of recharging/re-releasing cycles they can accomplish. A completely different scenario was observed with the experimental composites containing the FDCP fillers VS10 and VS20 in terms of PO release. These started releasing a significant ($p < 0.05$) amount of PO ions at the day 1, excluding VS10-5 % and VS20-5 % that had a delay in PO releasing. The experimental composites that presented the highest release of PO between 14 and 21 days of SBF immersion were VS20-10 %, VS10-20 % and VS20-20 %; this was probably due to the high concentration of the FDCP fillers in such materials. However, all the tested materials reached the maxim amount of PO accumulation at day 21 and there was no more significant accumulation of such ions up to 30 days of aging. In view of these results, it is possible to state that the tested experimental composites presented a relatively low and constant release up to 14 and 21 days. It is important to highlight that VS10-10 % and VS20-10 % showed a similar release of PO at day 7. Conversely, VS10-10 % showed at day 7 a greater release of Ca and a lower release of fluoride compared to VS20-10 %. Therefore, at such a specific period of incubation in SBF, there must have been a binding synergy between all those ions regulated by such a specific concentration of PO released by the experimental composites VS10-10 % and VS20-10 % and those present in the SBF; this may be the reason why a quick mineral deposition was observed in these two composites compared to all the other tested materials. Indeed, the analysis performed (FTIR-ATR and SEM/EDX) to evaluate the ability of the tested experimental composites to evoke surface' crystallisation showed that only VS10-10 % (Fig. 1G) and VS20-10 % (Fig. 1M) presented all the PO stretching of apatite peaks (559 cm^{-1}, 600 cm^{-1}, 962 cm^{-1}, 1021 cm^{-1}), along with other phosphate bands assigned to the phosphate group ($PO_{\nu 3}$: 1088 cm^{-1} and 1036 cm^{-1}) and P-O stretching vibration of PO_3^{2-}. Conversely, the CTR composite (Fig. 1E) after 30 days of SBF storage presented a FTIR spectra devoid of representative peaks of calcium phosphates, while all the other tested experimental composites presented after 15 days of SBF storage a spectra comparable to that observed with VS20-10 % and VS10-10 % at 7 days (Fig. 1). The only exception was VS20-5 % (Fig. 1L) that showed a clear presence of apatite-like precipitation only after 30 days of SBF storage. The results obtained in the current study during the FIB-SEM/EDX confirmed that VS20-5 % (Fig. 4B and B1) was able to form a consistent layer of plate-like crystals only after 30 days of SBF storage; they had a Ca/P

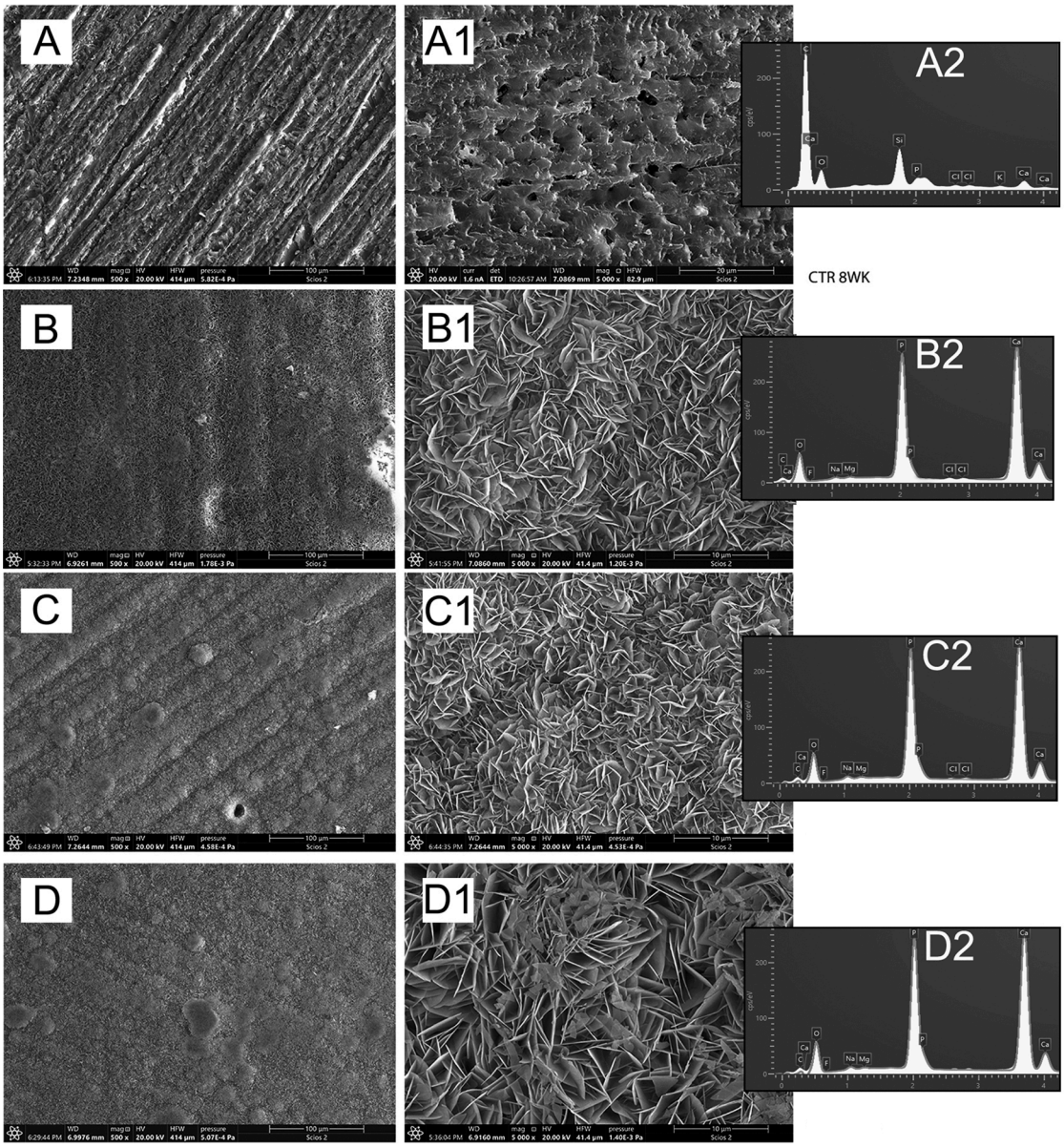

Fig. 3. A: Representative SEM micrograph of the composite control containing no FDCP showing a rough surface devoid of any presence of mineral crystals also at higher magnification (A1). The EDX analysis highlights no presence of Si from the glass filler, but Ca, P, Na, K, Mg and Cl, which were absorbed during 4 weeks of SBF storage (A2). B: Representative SEM micrograph of the experimental composite containing 5 % of the FDCP filler VS10 (VS10-5 %) after 15 days of SBF showing a completely covered by mineral crystals also at higher magnification (B1). In this case it possible to observe in the EDX spectra a clear presence of Ca and P from the new crystals formed on the resin's surface, along with Na, Mg and Cl, which were absorbed during SBF storage. Almost no fluoride is detected (B2). C: Representative SEM micrograph of the experimental composite containing 10 % of the FDCP filler VS10 (VS10-10 %) after 7 days of SBF showing a completely covered by mineral crystals also at higher magnification (B1). Also in this case, abundant Ca and P is detected from the new crystals deposited on the resin's surface, along with Na, Mg and Cl. The signal of fluoride is still very low (C2). D: Representative SEM micrograph of the experimental composite containing 20 % of the FDCP filler VS10 (VS10-20 %) after 15 days of SBF showing a completely covered by mineral crystals also at higher magnification (D1). Also in this case, abundant Ca and P is detected from the new crystals deposited on the resin's surface, along with Na, Mg and Cl. The signal of fluoride is almost absent in these crystals (C2).

ratio of 1.33 (Table 5), indicating the presence of octacalcium phosphate (OCP) [31], a well-known precursor of apatite [32,33]. It is hypothesised that such a delay in crystallisation in VS20-5 % may be due to a higher concentration of fluoride salts in the filler, compared to the VS10-5 %; such a condition may have hindered the formation of apatite-like crystals on the surface of such materials. Indeed, recent studies showed through ^{19}F MAS-NMR that the presence of high concentration of fluoride in calcium phosphate [22] and sodium-free bioactive glasses [34] could interfere with apatite deposition when immersed in SBF; it seems to occur especially when fluoride is present in concentration greater than 45 ppm [35,36].

Furthermore, the FIB-SEM/EDX confirmed the aforementioned FTIR results about the VS10-10 %, (Fig. 3C and C1) and VS20-10 % (Fig. 4C and C1), which had their surfaces completely covered by plate-like crystals (Ca/P ratio in both cases of 1.33) up to a level that the FTRI was not able to detect the characteristic peaks of the resin monomers typically observed in the CTR composite (Fig. 1A). Moreover, VS10-10 % and VS20-10 % were the only experimental composites that after 30 days of SBF storage showed plate-like crystals with a Ca/P of 1.35 (Table 5). This result indicates the maturation of OCP into calcium-deficient apatite [37,38]. However, the incomplete maturation to hydroxyapatite or to fluoride-containing apatite may be due to the SBF

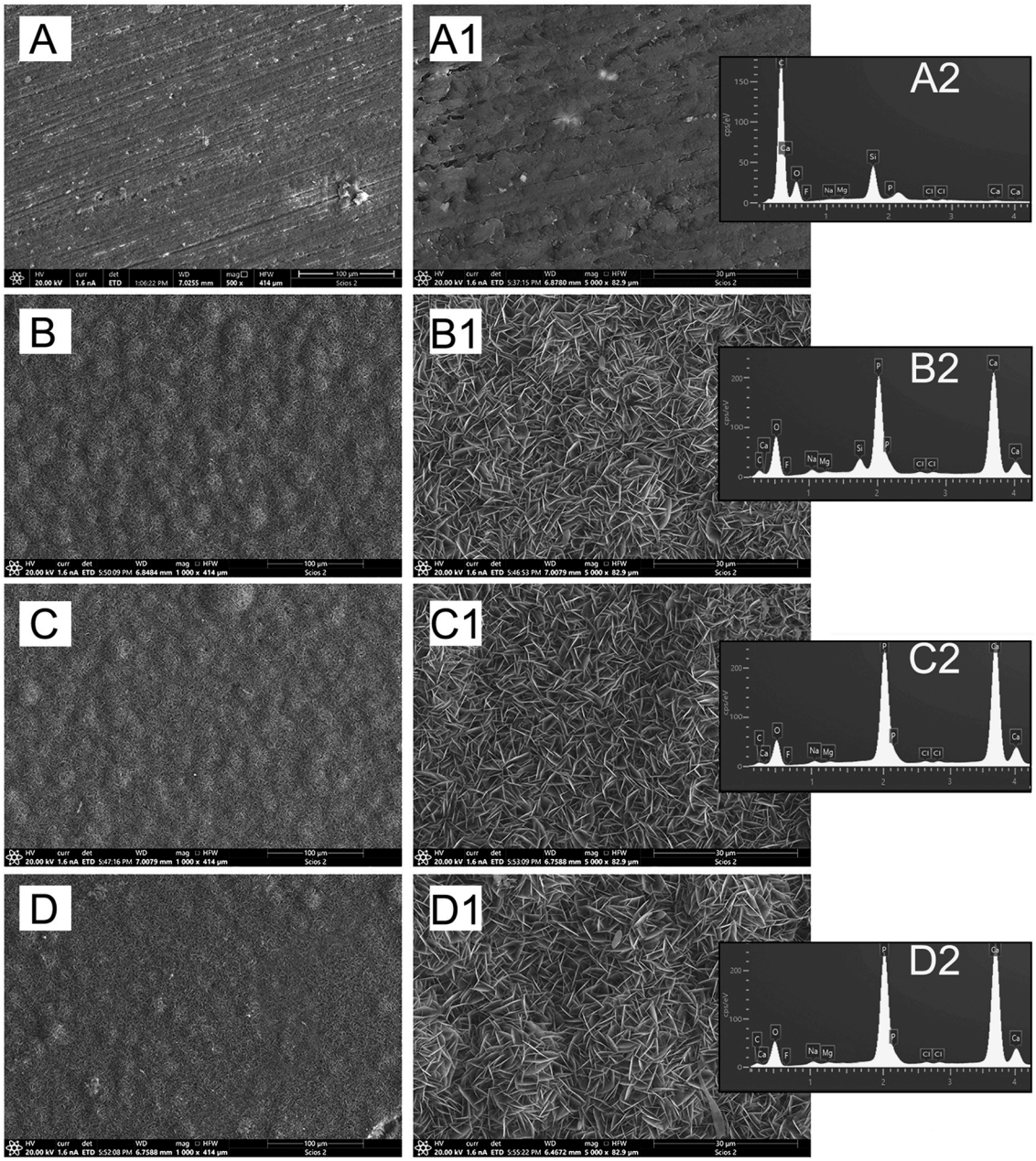

Fig. 4. A: Representative SEM micrograph of the experimental composite containing 5 % of the FDCP filler VS20 (VS20-5 %) after 15 days of SBF showing a rough surface devoid of any presence of mineral crystals also at higher magnification (**A1**). The EDX analysis highlights the presence of Si from the glass filler, but also some Ca, P, Na, Mg and Cl, which were absorbed during 4 weeks of SBF storage (A2). B: Representative SEM micrograph of the experimental composite containing 5 % of VS20 (VS20-5 %) after 30 days of SBF showing a surface completely covered by mineral crystals, clearly visible at higher magnification (B1). In this case it possible to observe in the EDX spectra a clear presence of Ca and P from the new crystals formed on the resin's surface, along with Na, Mg and Cl, which were absorbed during SBF storage. The signal of fluoride is almost absent in these crystals (B2). C: Representative SEM micrograph of the experimental composite containing 10 % of VS20 (VS20-10 %) after 7 days of SBF showing a surface totally covered by crystals, which are visible especially at higher magnification (C1). The EDX spectra shows a clear presence of Ca and P from the crystals deposited on the resin's surface, along with Na, Mg and Cl, absorbed during SBF storage. The signal of fluoride is very low (C2). D: Representative SEM micrograph of the experimental composite containing 20 % of the FDCP filler VS20 (VS20-20 %) after 15 days of SBF showing a resin's surface completely covered by crystals, which are clearly visible at higher magnification (D1). Also in this case, abundant Ca and P is detected from the such new crystals, along with Na, Mg and Cl. The signal for fluoride is still very low (D2).

solution used in this study [39].

Unfortunately, only a very low presence of fluoride was also observed in the EDX spectra of such experimental composites, so it is quite improbable that the crystals formed on their surfaces could actually be fluoride-containing apatite [40].

However, it has been recently reported [22] that FDCP fillers, especially those that incorporated a fluoride concentration of 5–10 wt% had the ability to convert into fluorapatite-like crystals after 30 d of immersion in SBF, while those incorporating high concentration of fluoride salts (20 wt%) were more prone to promote formation of CaF_2 after SBF immersion. Comparing these latter results and those obtained in this study, it is clear that once the FDCP are incorporated in a resin-matrix, which is subsequently polymerised, those lose part of their ability to convert into fluorapatite-like crystals with a Ca/P ratio of approx. 1.67.

Unfortunately, there is no available evidence that such a type of

Table 6
Release of UDMA, BisEMA and HEDA from the tested materials at 24 h (μg/mL).

	UDMA	HEDA	bisEMA
CTR (VS-free)	12.88 ± 1.28^{Aa}	$5.88 \pm 0.66^{A\ a}$	1.21 ± 0.40^{Aa}
VS10-5 %	$9.72 \pm 0.83^{B*}$	$3.15 \pm 0.78^{B*}$	$0.76 \pm 0.19^{A*}$
VS20-5 %	21.57 ± 3.61^{b}	6.20 ± 3.11^{a}	4.84 ± 1.37^{b}
VS10-10 %	$11.13 \pm 0.67^{A*}$	$3.84 \pm 0.35^{B*}$	$0.83 \pm 0.25^{A*}$
VS20-10 %	16.78 ± 0.84^{c}	4.64 ± 0.58^{a}	3.56 ± 0.18^{b}
VS10-20 %	$12.34 \pm 1.01^{A*}$	$3.87 \pm 0.40^{B*}$	$0.79 \pm 0.35^{A*}$
VS20-20 %	20.36 ± 5.12^{bc}	6.80 ± 4.25^{a}	6.07 ± 2.79^{b}

$^{(A.B.C.D)}$ Different uppercase letters indicate significance of monomer release (UDMA or HEDA or BisEMA) between the results obtained with composites having the same filler (VS10) at different concentration (R0 % to R20 %).
$^{(a.b.c)}$ Different uppercase letters indicate significance of monomer release (UDMA or HEDA or BisEMA) between the results obtained with composites having the same filler (VS20) at different concentration (R0 % to R20 %).
$^{(*)}$ symbol indicates significance in column of monomer release (UDMA or HEDA or BisEMA) between the results obtained with composites having different fillers (VS20 or VS10) but at the same concentration (5 % or 10 % or 20 %).

mineralisation attained with the experimental composites tested in this study may offer any particular protection against caries formation. Hence, further *in vitro* studies are necessary to evaluate the solubility of such crystals in acid environments and their potential role in remineralisation of mineral-depleted hard dental tissues. On the other hand, *in vivo* and clinical trials will be necessary to understand if such a sort of mineral precipitation can reduce the incidence of secondary caries, especially in composite-restored teeth. In our ongoing studies it is being investigated the bonding performance and the remineralising ability of such experimental composites once applied on simulated-caries lesion in dentine.

One more important aspect to consider after analysing the results obtained in the current study is the effect that incorporation of such FDCP fillers in resin-based materials had on the elution of resin monomers (e.g. UDMA, BisEMA and HEDA). This is important aspect as the elution of resin monomers into the oral cavity and/or into soft tissues (e.g. dental pulp, gingival and periodontal ligaments), along with the release of other chemical substances contained in dental biomaterials such as polymerisation initiation and catalysers, might cause serious biological issues in patients [41,42]. For instance, some *in vitro* studies [26,43] showed important cytotoxic, genotoxic, mutagenic or estrogenic effects and pulpal and gingival/oral mucosa reactions of monomers such as Bis-GMA eluted from dental composites.

The results obtained in the current study showed that all the composites containing the FDCP filler VS10 had a significant lower elution of resin monomers compared to the CTR and to the composites containing VS20 (Table 6). Thus, from this latter outcomes, VS10 results probably the most appropriate tested filler to be used for the formulation of innovative remineralising resin composites.

In general, it seems that the higher amount of fluoride ions released from "bioactive" fillers the greater the amount of monomers released resin-based materials due to a possible alteration of the resin matrix [44]. Furthermore, the presence of high concentration of fluoride in dimethacrylate-based materials may cause a reduction in mechanical strength compared to fluoride-free materials; this was potentially caused by a decrease of the polymer chain entanglement [45,46]. A high presence of fluoride ions can also induce oxidation of C=C bonds, so causing a critical deterioration of the polymer network with consequent increase of monomer's elution [47]. Release of fluoride ions may also favour hydrolytic degradation of the organosilicon ester group and silanol groups at the glass-filler/resin-matrix interface [48].

In the current study, it was also evaluated whether the incorporation of FDCP filler in experimental resin-based composite could offer any antibacterial properties against Gram+ primary colonisers of oral and dental surfaces such as *S. gordonii* [49]. The most relevant findings confirmed that the FCDP fillers used to formulate our experimental composites had a antimicrobial potency and especially when the percentage of such fillers was 10 wt% (VS10-10 % and VS20-10 %). Moreover, no significant difference was encountered between the experimental composites VS10-10 % and VS20-10 % (Figs. 5 and 6). Moreover, the LIVE/DEAD assay (Fig. 7), not only corroborated the selective response identified in the ATP and CFU assessment, but also indicated that VS10-10 % and VS20-10 % interfered with biofilm formation and growth.

It may be possible that a nonlinear correlation between the percentage of FDCP filler in the tested composites and the antimicrobial potency was in part due to a greater particle's agglomeration at concentration higher than FDCP >10 %. Thus, one can speculate that such a

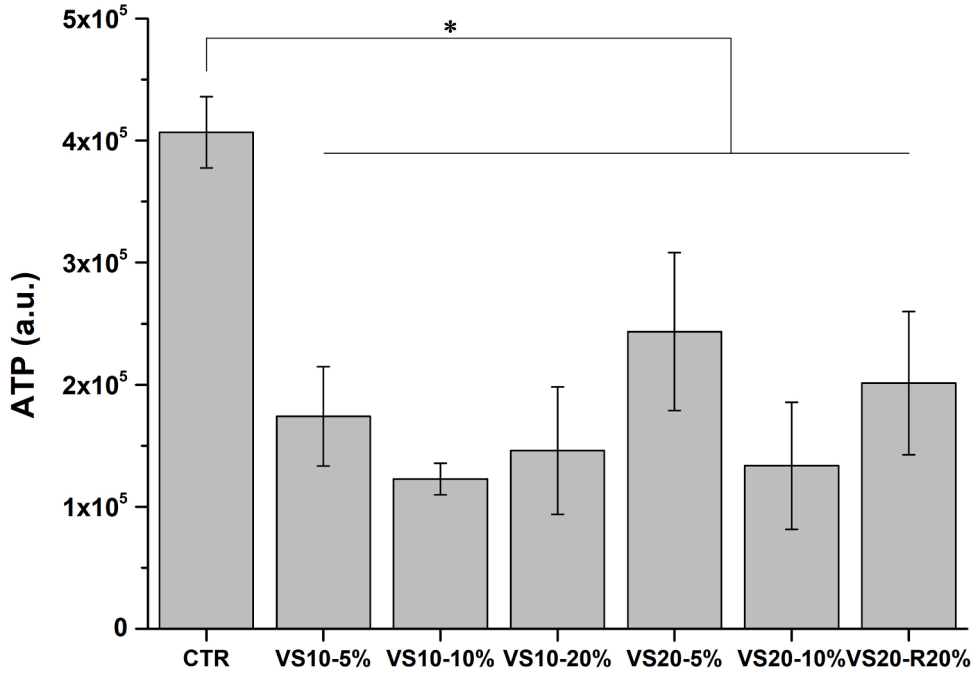

Fig. 5. ATP bioluminscence of *S. gordonii* cultured on different tested materials for 24 h at 37 °C.

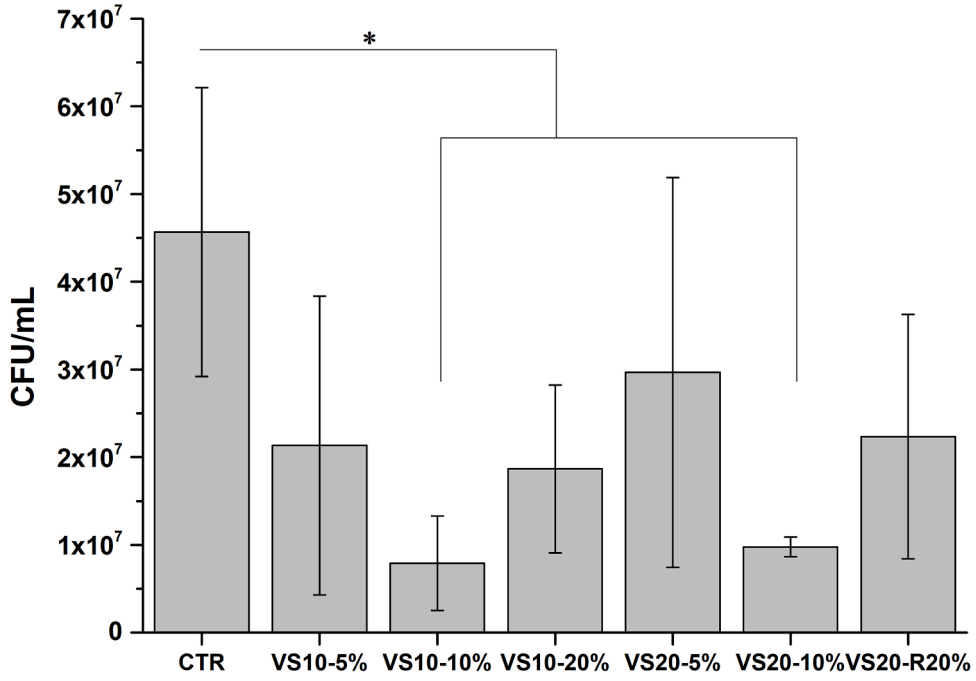

Fig. 6. CFU/mL of *S. ggordonii* grown after cultured on different tested materials for 24 h at 37 ºC.

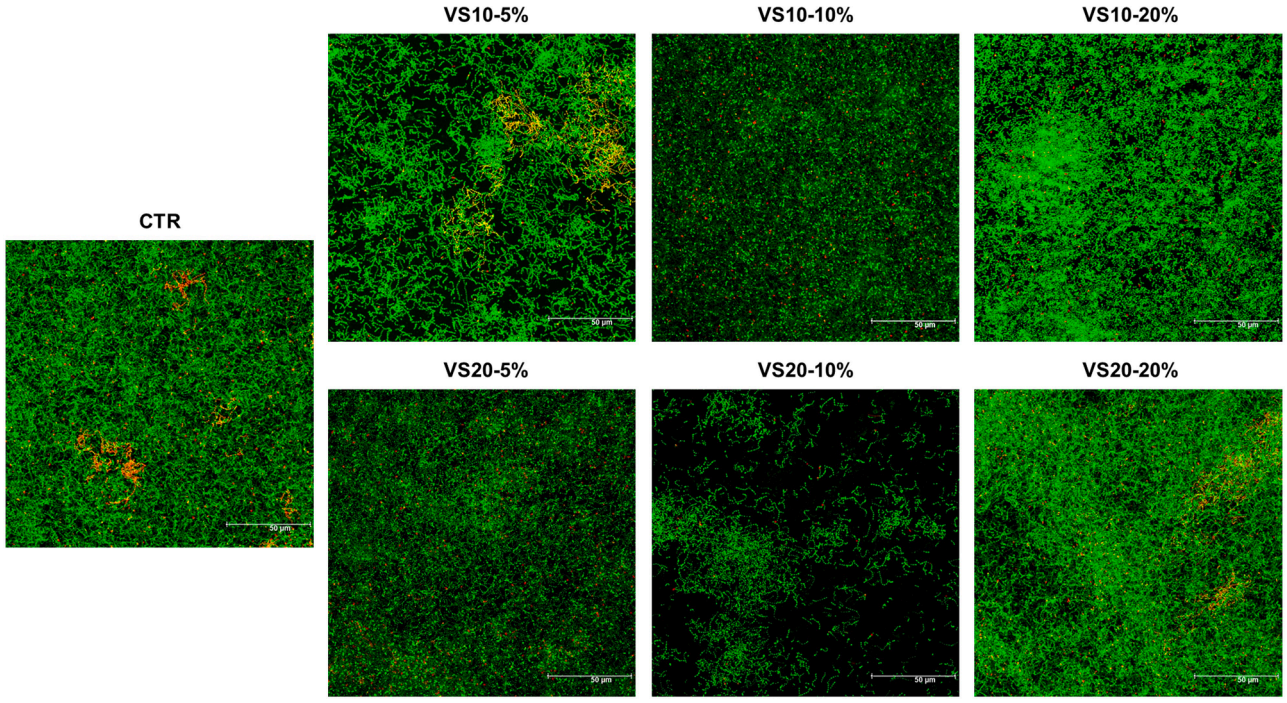

Fig. 7. Live/Dead micrographs of *S. gordonii* grown after cultured on different tested materials for 24 h at 37 ºC.

physical condition may have reduced the total effective area of the particles available to exert an antimicrobial effect on bacteria. Although the antibacterial effect of fluoride is well known, the results obtained during the microbiology tests demonstrated that having a FDCP filler with higher amount of fluoride salts within its composition (VS10 vs. VS20) did not offer any superior antimicrobial potency of the tested composites. Therefore, we hypothesise that the greater antibacterial activity observed in VS10-10 % and VS20-10 % was not only correlated to the presence of fluoride ions, but it was also correlated with their ability such composites to induce relatively quick mineral precipitation on their surfaces, as previous described. Indeed, it has been postulated that the presence of apatite-like crystals may interfere with the adhering affinity of some bacteria due to the formation of weak London–van der Waals forces and/or bridging forces [49,50]. This may represent a suitable method to create innovate remineralising materials with the ability to modulate the growth of bacteria on theirs surfaces without employing any substance with strong cytotoxic effect. Certainly, the fluoride-doped calcium phosphates tested in this study were shown to have less toxicity on hDPSCs and may induce more cell proliferation compared to a control fluoride-free calcium phosphate [22]. There are

evidence in the literature supporting the proliferation of human osteoblast-like cells increases in presence of fluoride-containing apatite, but in case of high concentration of fluoride ions it is likely to have an inhibition of cell growth [51]. Conversely, fluoride at low concentration presents low cytotoxicity and may promote biological activities in cells [51,52].

In conclusion, considering the limitation of this *in vitro* study and in view of the results obtained so far, it is possible to consider that the tested experimental composites containing fluoride-doped calcium phosphates may be promising restorative materials able to modulate bacteria growth, promote remineralisation and reduce the risk of cytotoxicity related to monomers' elution. As previously mentioned, further studies are needed to evaluate whether the application of such restorative materials after caries removal can be able to induce dentine remineralisation and improve the durability of dentine-bonded interfaces.

CRediT authorship contribution statement

Adrián M. Alambiaga-Caravaca: Writing – review & editing, Methodology, Investigation, Formal analysis. **Yu Fu Chou:** Visualization, Methodology, Investigation, Formal analysis. **Daniel Moreno:** Writing – review & editing, Formal analysis, Methodology. **Conrado Aparicio:** Writing – review & editing, Supervision, Methodology, Data curation, Conceptualization. **Alicia López-Castellano:** Writing – review & editing, Supervision, Methodology, Data curation, Conceptualization. **Victor Pinheiro Feitosa:** Writing – review & editing, Visualization, Formal analysis. **Arzu Tezvergil-Mutluay:** Writing – review & editing, Visualization, Methodology, Conceptualization. **Salvatore Sauro:** Writing – review & editing, Writing – original draft, Visualization, Validation, Supervision, Resources, Project administration, Methodology, Investigation, Funding acquisition, Formal analysis, Data curation, Conceptualization.

Declaration of competing interest

None of the authors have any conflict of interest with this study.

Acknowledgments

All authors gave their final approval and agree to be accountable for all aspects of the work. There is a patent on the calcium phosphates tailored with different concentrations of fluoride salts used in this study (ES2716942 - Composición y procedimiento para la obtención Y aplicación de un compuesto bioactivo que contiene fluoruro y el producto obtenido). The authors have no financial affiliation or involvement with any commercial organisation with direct financial interest in the materials discussed in this manuscript. This study was supported by the grant PID2020–120346GB-I00 funded by AEI/10.13039/501100011033 "Ministerio de Ciencia, Innovación y Universidades".

References

[1] J.E. Frencken, M.C. Peters, D.J. Manton, S.C. Leal, V.V. Gordan, E. Eden, Minimal intervention dentistry for managing dental caries - a review: report of a FDI task group, Int. Dent. J. 62 (2012) 223–243, https://doi.org/10.1111/IDJ.12007.

[2] F. Schwendicke, J. Frencken, N. Innes, Clinical recommendations on carious tissue removal in cavitated lesions, Monogr. Oral Sci. 27 (2018) 162–166, https://doi.org/10.1159/000487843.

[3] A. Banerjee, J.E. Frencken, F. Schwendicke, N.P.T. Innes, Contemporary operative caries management: consensus recommendations on minimally invasive caries removal, Br. Dent. J. 223 (3) (2017) 215–222, https://doi.org/10.1038/sj.bdj.2017.672.

[4] F. Schwendicke, C. Splieth, L. Breschi, A. Banerjee, M. Fontana, S. Paris, M. F. Burrow, F. Crombie, L.F. Page, P. Gatón-Hernández, R. Giacaman, N. Gugnani, R. Hickel, R.A. Jordan, S. Leal, E. Lo, H. Tassery, W.M. Thomson, D.J. Manton, When to intervene in the caries process? An expert Delphi consensus statement, Clin. Oral Investig. 23 (2019) 3691–3703, https://doi.org/10.1007/S00784-019-03058-W.

[5] M.K. Pugach, J. Strother, C.L. Darling, D. Fried, S.A. Gansky, S.J. Marshall, G. W. Marshall, Dentin caries zones: mineral, structure, and properties, J. Dent. Res. 88 (2009) 71–76, https://doi.org/10.1177/0022034508327552.

[6] D. Hashem, F. Mannocci, S. Patel, A. Manoharan, J.E. Brown, T.F. Watson, A. Banerjee, Clinical and radiographic assessment of the efficacy of calcium silicate indirect pulp capping: a randomized controlled clinical trial, J. Dent. Res. 94 (2015) 562–568, https://doi.org/10.1177/0022034515571415.

[7] D. Hashem, F. Mannocci, S. Patel, A. Manoharan, T.F. Watson, A. Banerjee, Evaluation of the efficacy of calcium silicate vs. glass ionomer cement indirect pulp capping and restoration assessment criteria: a randomised controlled clinical trial-2-year results, Clin. Oral Investig. 23 (2019) 1931–1939, https://doi.org/10.1007/S00784-018-2638-0.

[8] A.C. Ionescu, S. Hahnel, P. Delvecchio, N. Ilie, M. Moldovan, V. Zambelli, G. Bellani, E. Brambilla, Microbiological models for accelerated development of secondary caries in vitro, J. Dent. 127 (2022) 04333.

[9] J.L. Ferracane, Resin composite–state of the art, Dent. Mater. 27 (2011) 29–38, https://doi.org/10.1016/J.DENTAL.2010.10.020.

[10] A. Almahdy, F.C. Downey, S. Sauro, R.J. Cook, M. Sherriff, D. Richards, T. F. Watson, A. Banerjee, F. Festy, Microbiochemical analysis of carious dentine using Raman and fluorescence spectroscopy, Caries Res. 46 (2012) 432–440, https://doi.org/10.1159/000339487.

[11] S. Sauro, D.H. Pashley, Strategies to stabilise dentine-bonded interfaces through remineralising operative approaches – State of The Art, Int. J. Adhes. Adhes. 69 (2016) 39–57, https://doi.org/10.1016/J.IJADHADH.2016.03.014.

[12] M. Yoshiyama, J. Doi, Y. Nishitani, T. Itota, F.R. Tay, R.M. Carvalho, D.H. Pashley, Bonding ability of adhesive resins to caries-affected and caries-infected dentin, J. Appl. Oral Sci. 12 (2004) 171–176, https://doi.org/10.1590/S1678-77572004000300002.

[13] C.P. Isolan, R. Sarkis-Onofre, G.S. Lima, R.R. Moraes, Bonding to sound and Caries-Affected dentin: A systematic review and Meta-Analysis, J. Adhes. Dent. 20 (2018) 7–18, https://doi.org/10.3290/j.jad.a39775.

[14] Á.F. Cascales, A.P. Moscardó, M. Toledano, A. Banerjee, S. Sauro, An *in-vitro* investigation of the bond strength of experimental ion-releasing dental adhesives to caries-affected dentine after 1 year of water storage, J. Dent. 119 (2022), https://doi.org/10.1016/J.JDENT.2022.104075.

[15] P. Maciel Pires, A.C. Ionescu, M.T. Pérez-Gracia, E. Vezzoli, I.P.M. Soares, E. Brambilla, A. de Almeida Neves, S. Sauro, Assessment of the remineralisation induced by contemporary ion-releasing materials in mineral-depleted dentine, Clin. Oral Investig. 26 (2022) 6195–6207, https://doi.org/10.1007/S00784-022-04569-9.

[16] P.M.I. Pires, A.S. Nunes Monteiro, P. Helena De Accioly Costa, A.S. Silva, R. T. Lopes, K. Yoshihara, S. Sauro, A. De Almeida Neves, Dentine mineral changes induced by polyalkenoate cements after different selective caries removal techniques: an *in vitro* study, Caries Res. 57 (2023) 21–31, https://doi.org/10.1159/000529101.

[17] Y. Liu, N. Li, Y. Qi, L.N. Niu, S. Elshafiy, J. Mao, L. Breschi, D.H. Pashley, F.R. Tay, The use of sodium trimetaphosphate as a biomimetic analog of matrix phosphoproteins for remineralization of artificial caries-like dentin, Dent. Mater. 27 (2011) 465–477, https://doi.org/10.1016/J.DENTAL.2011.01.008.

[18] M. Giannini, S. Sauro, Bioactivity" in restorative dentistry: standing for the use of innovative materials to improve the longevity of restorations in routine dental practice, J. Adhes. Dent. 23 (2021) 176–178, https://doi.org/10.3290/J.JAD.B1179733.

[19] A.C. Ionescu, S. Hahnel, G. Cazzaniga, M. Ottobelli, R.R. Braga, M.C. Rodrigues, E. Brambilla, Streptococcus mutans adherence and biofilm formation on experimental composites containing dicalcium phosphate dihydrate nanoparticles, J. Mater. Sci. Mater. Med. 28 (2017), https://doi.org/10.1007/S10856-017-5914-7.

[20] H. Mitwalli, R. AlSahafi, E.G. Albeshir, Q. Dai, J. Sun, T.W. Oates, M.A.S. Melo, H. H.K. Xu, M.D. Weir, Novel nano calcium fluoride remineralizing and antibacterial dental composites, J. Dent. 113 (2021), https://doi.org/10.1016/J.JDENT.2021.103789.

[21] M.C. Peters, E. Bresciani, T.J.E. Barata, T.C. Fagundes, R.L. Navarro, M.F. L. Navarro, S.H. Dickens, *In vivo* dentin remineralization by calcium-phosphate cement, J. Dent. Res. 89 (2010) 286–291, https://doi.org/10.1177/0022034509360155.

[22] S. Sauro, G. Spagnuolo, C. Del Giudice, D.M.A. Neto, P.B.A. Fechine, X. Chen, S. Rengo, X. Chen, V.P. Feitosa, Chemical, structural and cytotoxicity characterisation of experimental fluoride-doped calcium phosphates as promising remineralising materials for dental applications, Dent. Mater. 39 (2023) 391–401, https://doi.org/10.1016/J.DENTAL.2023.03.007.

[23] H.W. Kim, H.E. Kim, J.C. Knowles, Fluor-hydroxyapatite sol–gel coating on titanium substrate for hard tissue implants, Biomaterials 25 (2004) 3351–3358, https://doi.org/10.1016/J.BIOMATERIALS.2003.09.104.

[24] T. Kokubo, H. Kushitani, S. Sakka, T. Kitsugi, T. Yamamuro, Solutions able to reproduce *in vivo* surface-structure changes in bioactive glass-ceramic A-W, J. Biomed. Mater. Res. 24 (1990) 721–734, https://doi.org/10.1002/JBM.820240607.

[25] R. Łagocka, M. Mazurek-Mochol, K. Jakubowska, M. Bendyk-Szeffer, D. Chlubek, J. Buczkowska-Radlińska, Analysis of base monomer elution from 3 flowable bulk-fill composite resins using high performance liquid chromatography (HPLC), Med. Sci. Monit. 24 (2018) 4679, https://doi.org/10.12659/MSM.907390.

[26] A.M. Alambiaga-Caravaca, A. López-Castellano, Y.F. Chou, A. Luzi, J.M. Núñez, A. Banerjee, M. del M. Jovani Sancho, S. Sauro, Release kinetics of monomers from dental composites containing fluoride-doped calcium phosphates, Pharmaceutics 15 (15) (2023) 1948, https://doi.org/10.3390/PHARMACEUTICS15071948.

[27] M.A. Cebe, F. Cebe, M.F. Cengiz, A.R. Cetin, O.F. Arpag, B. Ozturk, Elution of monomer from different bulk fill dental composite resins, Dent. Mater. 31 (2015) e141–e149, https://doi.org/10.1016/j.dental.2015.04.008.
[28] W. Jiang, Z. Xie, S. Huang, Q. Huang, L. Chen, X. Gao, Z. Lin, Targeting cariogenic pathogens and promoting competitiveness of commensal bacteria with a novel pH-responsive antimicrobial peptide, J. Oral Microbiol. 15 (2022), https://doi.org/10.1080/20002297.2022.2159375.
[29] A. Besinis, R. Van Noort, N. Martin, Remineralization potential of fully demineralized dentin infiltrated with silica and hydroxyapatite nanoparticles, Dent. Mater. 30 (2014) 249–262, https://doi.org/10.1016/J.DENTAL.2013.11.014.
[30] H. Mitwalli, R. AlSahafi, A. Alhussein, T.W. Oates, M.A.S. Melo, H.H.K. Xu, M. D. Weir, Novel rechargeable calcium fluoride dental nanocomposites, Dent. Mater. 38 (2022) 397–408, https://doi.org/10.1016/J.DENTAL.2021.12.022.
[31] W. Cao, J. Jin, G. Wu, N. Bravenboer, M.N. Helder, E.A.J.M. Schulten, R. G. Bacabac, J.L. Pathak, J. Klein-Nulend, Kappa-carrageenan-Functionalization of octacalcium phosphate-coated titanium Discs enhances pre-osteoblast behavior and osteogenic differentiation, Front. Bioeng. Biotechnol. 10 (2022) 1011853, https://doi.org/10.3389/FBIOE.2022.1011853/BIBTEX.
[32] M.S.A. Johnsson, G.H. Nancollas, The role of brushite and octacalcium phosphate in apatite formation, Crit. Rev. Oral Biol. Med. 3 (1992) 61–82, https://doi.org/10.1177/10454411920030010601.
[33] V.P. Feitosa, M.G. Bazzocchi, A. Putignano, G. Orsini, A.L. Luzi, M.A.C. Sinhoreti, T.F. Watson, S. Sauro, Dicalcium phosphate ($CaHPO_4{\cdot}2H_2O$) precipitation through ortho- or meta-phosphoric acid-etching: effects on the durability and nanoleakage/ultra-morphology of resin-dentine interfaces, J. Dent. 41 (2013) 1068–1080, https://doi.org/10.1016/J.JDENT.2013.08.014.
[34] D.S. Brauer, N. Karpukhina, R.V. Law, R.G. Hill, Structure of fluoride-containing bioactive glasses, J. Mater. Chem. 19 (2009) 5629–5636, https://doi.org/10.1039/B900956F.
[35] D.S. Brauer, N. Karpukhina, M.D. O'Donnell, R.V. Law, R.G. Hill, Fluoride-containing bioactive glasses: effect of glass design and structure on degradation, pH and apatite formation in simulated body fluid, Acta Biomater. 6 (2010) 3275–3282, https://doi.org/10.1016/J.ACTBIO.2010.01.043.
[36] N.R. Mohammed, N.W. Kent, R.J.M. Lynch, N. Karpukhina, R. Hill, P. Anderson, Effects of fluoride on *in vitro* enamel demineralization analyzed by ^{19}F MAS-NMR, Caries Res. 47 (2013) 421–428, https://doi.org/10.1159/000350171.
[37] Q. Yang, T. Troczynski, D.M. Liu, Influence of apatite seeds on the synthesis of calcium phosphate cement, Biomaterials 23 (2002) 2751–2760, https://doi.org/10.1016/S0142-9612(02)00010-8.
[38] M. Andrés-Vergés, C. Fernández-González, M. Martínez-Gallego, J.D. Solier, I. Cachadiña, E. Matijević, A new route for the synthesis of calcium-deficient hydroxyapatites with low Ca/P ratio: both spectroscopic and electric characterization, J. Mater. Res. 15 (2000) 2526–2533, https://doi.org/10.1557/JMR.2000.0362/METRICS.
[39] J. Yun, K.H. Tsui, Z. Fan, M. Burrow, J.P. Matinlinna, Y. Wang, J.K.H. Tsoi, A biomimetic approach to evaluate mineralization of bioactive glass-loaded resin composites, J. Prosthodont. Res. 66 (2022) 572–581, https://doi.org/10.2186/jpr.JPR_D_21_00177.
[40] R.J.M. Lynch, R. Navada, R. Walia, Low-levels of fluoride in plaque and saliva and their effects on the demineralisation and remineralisation of enamel; role of fluoride toothpastes, Int. Dent. J. 54 (2004) 304–309, https://doi.org/10.1111/J.1875-595X.2004.TB00003.X.
[41] D. Khvostenko, T.J. Hilton, J.L. Ferracane, J.C. Mitchell, J.J. Kruzic, Bioactive glass fillers reduce bacterial penetration into marginal gaps for composite restorations, Dent. Mater. 32 (2016) 73–81, https://doi.org/10.1016/J.DENTAL.2015.10.007.
[42] W. Geurtsen, Substances released from dental resin composites and glass ionomer cements, Eur. J. Oral Sci. 106 (1998) 687–695, https://doi.org/10.1046/J.0909-8836.1998.EOS10602II04.X.
[43] N.H. Kleinsasser, K. Schmid, A.W. Sassen, U.A. Harréus, R. Staudenmaier, M. Folwaczny, J. Glas, F.X. Reichl, Cytotoxic and genotoxic effects of resin monomers in human salivary gland tissue and lymphocytes as assessed by the single cell microgel electrophoresis (Comet) assay, Biomaterials 27 (2006) 1762–1770, https://doi.org/10.1016/J.BIOMATERIALS.2005.09.023.
[44] A. Zitz, I. Gedalia, R. Grajower, Addition of fluoride compounds to acrylic resin plates: bending strength and fluoride release, J. Oral Rehabil. 8 (1981) 37–41, https://doi.org/10.1111/J.1365-2842.1981.TB00473.X.
[45] J.W. Stansbury, J.M. Antonucci, Dimethacrylate monomers with varied fluorine contents and distributions, Dent. Mater. 15 (1999) 166–173, https://doi.org/10.1016/S0109-5641(99)00028-7.
[46] L. Papagiannoulis, J. Tzoutzas, G. Eliades, Effect of topical fluoride agents on the morphologic characteristics and composition of resin composite restorative materials, J. Prosthet. Dent. 77 (1997) 405–413, https://doi.org/10.1016/S0022-3913(97)70166-5.
[47] E.P.P lueddemann, Adhesion through silane coupling agents, J. Adhes. 2 (1970) 184–201, https://doi.org/10.1080/0021846708544592.
[48] J. Kreth, J. Merritt, F. Qi, Bacterial and host interactions of oral streptococci, DNA Cell Biol. 28 (2009) 397–403, https://doi.org/10.1089/dna.2009.0868.
[49] X. Zheng, P.J. Arps, R.W. Smith, Adhesion of two bacteria onto dolomite and apatite: their effect on dolomite depression in anionic flotation, Int. J. Miner. Process. 62 (2001) 159–172, https://doi.org/10.1016/S0301-7516(00)00050-8.
[50] M.C. van Loosdrecht, J. Lyklema, W. Norde, G. Schraa, A.J. Zehnder, The role of bacterial cell wall hydrophobicity in adhesion, Appl. Environ. Microbiol. 53 (1987) 1893–1897, https://doi.org/10.1128/AEM.53.8.1893-1897.1987.
[51] J.L. Kyzer, M. Martens, Metabolism and toxicity of fluorine compounds, Chem. Res. Toxicol. 34 (2021) 678–680, https://doi.org/10.1021/ACS.CHEMRESTOX.0C00439/ASSET/IMAGES/MEDIUM/TX0C00439_0001.GIF.
[52] W.K. Hagmann, The many roles for fluorine in medicinal chemistry, J. Med. Chem. 51 (2008) 4359–4369, https://doi.org/10.1021/JM800219F/ASSET/JM800219F.FP.PNG_V03.